The cooling potential of Rain Gardens and Green Roofs

- The influence on energy partitioning in Kvillebäcken, Gothenburg

Julia Cederbrant

Degree of Master of Science (120 credits)
with a major in Geography
30 hec

Department of Earth Sciences
University of Gothenburg
2021 B1129

Faculty of Science

UNIVERSITY OF GOTHENBURG

UNIVERSITY OF GOTHENBURG
Department of Earth Sciences
Geovetarcentrum/Earth Science Centre

The cooling potential of Rain Gardens and Green Roofs

- The influence on energy partitioning in Kvillebäcken, Gothenburg

Julia Cederbrant

ISSN 1400-3821

B1129
Master of Science (120 credits) thesis
Göteborg 2021

Mailing address
Geovetarcentrum
S 405 30 Göteborg

Address
Geovetarcentrum
Guldhedsgatan 5A

Telephone
031-786 19 56

Geovetarcentrum
Göteborg University
S-405 30 Göteborg
SWEDEN

Abstract

Blue-green infrastructure (BGI) has become a popular way of combating the effects of climate change, both regarding heat mitigation and runoff from precipitation. This thesis aims to understand the potential of two BGI types, namely rain gardens and green roofs, of increasing the latent heat fraction in an urban area and thereby also understand the possible cooling effect from these measures. Rain gardens and green roofs are further compared to the effect on energy partitioning of high albedo roofs and an increased surface fraction of grass in the Kvillebäcken area in Gothenburg. The thesis was performed using an energy and water balance model called SUEWS in order to investigate heat and water fluxes. Scenarios of increased rain garden and green roof surface coverage was used to model the influence on latent and sensible heat fluxes. Results show that both rain gardens and green roofs have potential to increase latent heat and thereby reduce temperatures. However, both BGI-solutions increase latent heat during periods of frequent precipitation and not when it is needed the most, that is during heatwaves and periods of strong Urban Heat Island (UHI). Increasing grass areas have a larger effect than other BGI but is commonly outcompeted in urban areas due to lack of space, making it a less attractive option in densely built areas. During dry and hot periods, it was found that high albedo roofs have the largest potential to decrease temperatures, however through a reduction of sensible heat. The study concludes that water availability is crucial for BGI to increase latent heat, as water needs to be frequently added for maximum efficiency. To combine the varied benefits of BGI with high albedo surfaces should therefore give the largest effect on cooling the urban climate.

Key words: *urban energy balance, urban water balance, SUEWS, energy partitioning, Blue-green infrastructure*

Acknowledgements

This thesis marks the end of a 5 yearlong educational journey, and also the end of a 30-credit master thesis course as the last part of the Master program in Geography at the University of Gothenburg. I would like to start this acknowledgement by thanking my fellow master students for encouragement, support and overall pleasant company during these last two years.

I would like to thank my supervisor Associate Professor Fredrik Lindberg for guidance and input along the way. My warmest thanks also go to PhD Oskar Bäcklin for endless hours of zoom support and encouragement in moments of "I will never get this stupid code to work". Thank you both, for your patience and for believing in me even though I am far from a natural when it comes to programming.

Further, I would like to thank Professor Sue Grimmond and Dr Ting Sun who have guided me through problems arising when modelling in SUEWS.

Finally, many thanks to my paternal grandparents for the effort of proofreading this thesis and spending hours and hours on finding the slightest misspelling.

Julia Cederbrant
May 21, 2021

Table of Contents

1. Introduction

Most urban areas in the world face similar challenges of hosting a rapidly increasing population at the same time as the effects of climate change are becoming more evident (Yu et al., 2020). Urbanization transforms the landscape, altering natural surfaces into impervious materials which not only reduces infiltration possibilities for precipitation, but also changes energy and radiation balances (Oke et al., 2017). In a changing climate with more frequent and intense heatwaves, the impervious surfaces of the city intensify the already severe effects of climate change (Yu et al., 2020; Miao, Chen., 2014). Urban materials, such as concrete and asphalt, have a larger potential to store heat for longer periods of time than natural materials (Miao, Chen., 2014). This contributes to the effect known as Urban Heat Island (UHI) which is the phenomenon where an urban area is warmer than its rural surroundings, especially at night (Yu et al, 2020). Heatwaves and UHI does not only compromise the thermal comfort in an urban area but are also a health risk (Völker et al., 2013; Oke et al., 2017). Exposure to excessive heat can, for sensitive groups such as elderly people, cause heat rashes, heat cramps or even fatal heart strokes (Völker et al., 2013) which is why it is important to understand how different materials and structures affect heat fluxes within the urban environment.

To understand what affects the urban climate and to be able to control it in a better way is becoming more important every year. To do so, it is fundamental to recognize the very basics of urban heat exchanges, namely the surface energy balance (SEB). The SEB can be applied to a variety of spatial and temporal scales and is key for understanding energy transfer and storage, not only within the urban dimension but also between the urban area and the different layers of the atmosphere (Oke et al., 2017). Connected to the SEB is the hydrological cycle, which is highly modified in urban areas as an effect of the urban structure. The urban fabric tends to consist of a large share of impervious surfaces. Therefore, water runs on top of the surface material as runoff (ibid.). This creates a need to transport water away from the urban surfaces in order to avoid flooding and a common solution are storm water systems. These tend to be highly efficient, and water is rapidly transported away into underground pipes (ibid.). Although efficient, this gives no time to use the water's natural cooling effect through evaporation, which affects the energy balance of the urban area.

There are a variety of strategies used in urban planning in order to minimize the consequences of heat stress and flooding in urban areas, and many strategies try to mimic the natural systems. Strategies using blue and green elements have received attention during later years for being an efficient solution for reducing urban temperatures (Yu et al., 2020), known as Blue-green infrastructure (BGI). These strategies are assumed to increase cooling due to several factors, where changes of albedo and evaporative cooling are two of the most important (Hathway & Sharples, 2012; Žuvela-Aloise et al., 2016). However, there are drawbacks considering the requirement of maintenance in order to function to its full potential, which result in BGI possibly being a rather expensive measure (Gothenburg University, 2021; SMHI, 2019). It is therefore important to evaluate their function, especially for less researched areas, such as the potential of temperature reduction on a neighborhood scale. Previous research on BGIs potential to affect latent and sensible heat flux has mostly been conducted in temperate regions (T. Sun et al., 2016). Thus, this study investigates BGI function on energy partitioning in a high latitude city like Gothenburg.

1.1 Aim

The aim of this thesis is to model the potential of rain gardens and green roofs to affect the energy partitioning, and thereby the potential to reduce temperature in an urban environment on a neighborhood scale. The following research questions guides the study:

- How do rain gardens and green roofs affect the energy partitioning?
- What effect does rain gardens and green roofs have on the energy partitioning during periods of different weather conditions?
- What other measures could be taken to enhance or complement the temperature reducing potential of rain gardens and green roofs?

In order to fulfil the aim, the area of Kvillebäcken in Gothenburg was selected. To have Eastern Kvillebäcken as a research area allows for a detailed neighborhood scale but yet with a variety of urban characteristics; impervious surface intertwined with blue-green infrastructure.

2. Background

2.1 Energy balance

The starting point of understanding the urban climate on a larger scale is to understand the influence that the urban fabric has on the Surface Energy Balance (SEB) (Oke et al., 2017). The urban environment can be investigated on many scales, from individual buildings to neighborhoods and blocks (ibid.). The SEB of urban areas tend to differ quite drastically from its rural surroundings due to the different radiative properties of impermeable surfaces, such as buildings and asphalt, but also due to actions of inhabitants in the city such as combustion from motorized vehicles and heating of housing (Erell, Pearlmutter, & Williamson, 2012). Different surface characteristics like albedo, roughness length or availability of moisture decides the partitioning of the energy balance (Christen & Vogt, 2004). However, even though individual structures or buildings each have their own radiation balance, it is not interesting to investigate them separately since it is the joint effect of all surfaces that affect the local climate. Instead, one must understand how they interact with all other elements of the neighborhood and the city (Oke et al., 2017).

2.1.1 Urban Energy Balance

The Urban Energy Balance (UEB) where all parameters are expressed in the unit of [W m−2] (watts per square meters) (Alexander et al., 2016) and can be described as:

$$Q^* + Q_F = Q_H + Q_E + \Delta Q_S \, (+ \Delta Q_A) \qquad [\mathrm{W\ m{-}2}]$$

$$Q^* = K_{\downarrow} + K_{\uparrow} + L_{\downarrow} + L_{\uparrow}$$

where **Q*** is net all wave radiation (Erell, Pearlmutter, & Williamson, 2012). Q* is the sum of incoming and outgoing longwave (L) and shortwave (K) radiation in the following equation, where (↑) represent outgoing radiation and (↓) represent incoming radiation (Christen & Vogt, 2004). Q* is dominated by shortwave incoming radiation during daytime and longwave outgoing radiation at nighttime (Oke, 1987). This means that Q* is positive during daytime and negative during nighttime.

Q_F is the anthropogenic heat flux, which can have more or less impact on the total urban energy balance. In a cold region during winters, when incoming solar radiation is small and extensive heating of housing occurs, Q_F contributes to a large share of the input of energy into the balance (Taha, 1997). Population data is used to estimate the anthropogenic influence on the urban energy balance (Järvi et al, 2011). The anthropogenic heat flux cannot be observed directly, and is instead commonly estimated as follows (Grimmond, 1992; Sailor and Lu, 2004):

$$Q_F = Q_V + Q_B + Q_M$$

where Q_F stands for the total anthropogenic heat flux and is estimated from three parameters. Q_v represents heat released from vehicles and Q_B is heat released from buildings. Q_M, which usually is negligible in comparison to the former two, is heat released from human metabolism (Sailor & Lu, 2004). Population, and thereby also Q_F, tends to differ over the day and depending on what area that is investigated it will look differently (Bergroth, 2019).

ΔQ_s represents the net storage of heat in urban materials, including buildings, trees or different ground materials (Erell, Pearlmutter, & Williamson, 2010). ΔQ_A stands for net energy added to or removed from the urban area by wind (ibid.;Ward et al., 2016) referred to as advection. This variable is usually included in the UEB but is avoided in models, due to the assumption of a relatively homogenous urban surface (Oke et al., 2017) where advection effects are negligible (Alexander et al., 2016).

Q_H stands for the sensible heat flux, which is the energy exchange between the urban structure and the air immediately above it, when there is a temperature difference between the two (Ward et al., 2016;Errel, Pearlmutter & Williamson, 2010). The rate of Q_H is affected by the difference in temperature between the air and the surface, and also by the resistance to heat transfer between the surface and the air (Erell, Pearlmutter & Williamson, 2010).

Q_E is the latent heat flux, which is energy required or being released when a substrate changes temperature and also goes through a phase change. For example, when water goes from liquid to gas (Oke et al., 2017;Ward et al., 2016). One concrete example is when a plant transpires, taking up water in liquid form from the soil and releasing it into the atmosphere in gas form.

This phase change requires energy which is taken from the surrounding atmosphere, resulting in an air temperature decrease (Gkatsopoulos, 2017). The possibility of latent heat to form is important for heat mitigation, since availability of water and vegetation is the foundation of evapotranspiration, which in the end lowers air temperature. Latent heat is present in urban areas through evaporation and transpiration from vegetation and can during optimal conditions lower temperatures by several degrees in so called 'oases' made up by parks and other green areas, meaning an area that is cooler than their surroundings (Taha, 1997). The urban structure generally has more runoff and a larger drainage capacity than the rural surroundings, where water in urban areas is removed either by going down into pipes or quickly evaporating from the many impervious surfaces of the urban environment (ibid.). Less surface water is therefore available for evapotranspiration, and the cooling effect of Q_E in cities is weak (ibid.).

2.1.2 The relationship between Q_H and Q_E

The relationship between Q_H and Q_E is strong but complex, where one can, simplified, state that Q_H is a warming agent while Q_E acts cooling for the surrounding air mass (Oke et al., 2017). If Q_H is high, the lower atmosphere is warmer whilst if Q_E is high, the air is more humid which means that the surface air is cooler (ibid.). The two fluxes always add up to a total of one, meaning that when Q_H is high, Q_E is low and vice versa (ibid.). This means that one flux is always increasing at the expense of the other, and through evapotranspiration the solar energy is converted into latent rather than sensible heat, which reduces the heat gain (Konarska et al., 2013).

2.1.3 Available Energy

The available energy equation is based on the UEB but rearranged, however still with each side of the equation representing the total available energy (Oke et al., 2017). The net storage of heat in urban materials (ΔQs) has been shifted to be a part of the left side of the UEB equation:

$$Q^* + Q_F - \Delta Q_S = Q_E + Q_H$$

In this equation ΔQ_A has been removed due to its negligible effect. Available energy (AE) can be presented as stated in the below equation:

$$AE = Q_E + Q_H$$

The following equation has been used in order to calculate partitioning of Q_E and Q_H of Available Energy (AE) to understand when one flux is higher than the other:

$$Q_E \text{ fraction of } AE = Q_E / (AE)$$

2.2 Urban Water Balance

The Urban Water Balance (UWB) differs from its rural counterpart due less greenery and a larger share of impermeable surfaces in urban areas (Oke et al., 2017). These modifications alter both soil moisture and evaporation as well as increase the amount and the speed of runoff water (ibid.). The UWB can be described as:

$$P + I + F = R + E + \Delta S$$

Where *P* stands for precipitation. *I* is imported water, for example from piped water. *F* is water that forms through combustion in vehicles and industry (Oke et al., 2017). *R* represents runoff, meaning precipitation that is not infiltrated into the ground and thereby moves over land (T. Sun & Grimmond, 2019). *E* stands for evaporation and ΔS is net change in water storage (ibid.). Generally, there is only a small amount of the received precipitation in an urban area that stays on the surface until it evaporates. Most of it is removed efficiently by drainage pipes that are

connected to the sewer system, meaning that it has been removed from the energy equation of the urban area (Oke et al., 2017). In order for cities to handle water sustainably, the implementation of BGI is commonly used today with the aim of runoff detention at the same time as moisture availability is kept high. Implementing BGI may therefore counteract the tendencies of urban areas to be dry and to mainly contribute to the sensible heat flux (ibid.).

2.3 Urban Climate

The urban climate differs from the rural surroundings and is highly influenced by the urban structure (Oke et al., 2017). Both the type of material and the way that urban elements are located affect the urban climate, and by planning strategically one can enhance or reduce the effects these elements have on the local climate (Coutts et al., 2007). Material used to build the urban area affects the energy balance (more closely described in section 2.1), which in the extended perspective controls the urban temperature. Urban elements consists of materials that are not present in a rural area and are traditionally darker, meaning that they have a high albedo and commonly a high emittance (Erell, Pearlmutter & Williamson, 2010). This results in that much of the incoming radiation is absorbed into the urban fabric and is stored during the day when incoming radiation is still present (Oke et al., 2017).

2.3.1 Surface cover material

Materials in the urban landscape have different properties which determine how they react to radiation, resulting in diversity in surface energy balance among these materials (Erell, Pearlmutter & Williamson, 2010). Building roofs are one type of facet that to a larger extent occurs in the urban area and that normally are built in a way that makes them absorb a large part of the solar radiation, resulting in high surface temperatures (ibid.). Since roofs commonly are built to lead away precipitation, they tend to dry up quickly after rainfalls. Therefore, the main energy emitted from roofs is sensible heat (Q_H). Looking at more vegetated urban areas, such as fields of grass where more moisture is available, the latent heat (Q_E) will make up a larger fraction than Q_H of the total energy available (Oke et al., 2017). This demonstrates the importance of moisture availability for the possibility of incoming energy transforming into latent heat (Mieli et al., 2020).

2.3.2 Urban Heat Island

When the incoming radiation ceases at dusk, energy stored in building material will be released, contributing to the effect known as the Urban Heat Island (UHI) which normally is at its strongest at night (Oke et al., 2017). This phenomenon can affect an urban area at different levels. Below the ground, at the surface and in different urban atmospheric layers, but it always implies a higher temperature in the urban area than its rural surroundings (ibid.). The effects of UHI puts people living in urban areas in a vulnerable position, which is increasingly urgent since more people than ever live in urban areas (Heaviside et al., 2017). Further, extended periods of hot weather and heatwaves have become more frequent in recent years and will increase in both length and intensity in the future (Handmer et al., 2018 IPCC). During heatwaves urban areas experience a double effect, with the high temperatures from the heatwave itself and with the added heat from the UHI effect (Gunawardena et al., 2017).

What further enhances the UHI effect in urban areas is the efficient storm drains commonly used in cities, where precipitation and runoff is led down into pipes below ground and transported away from the city. This inhibits precipitation to evaporate and thereby reduces the moisture availability and evaporative cooling (Taha, 1997). Lastly, anthropogenic heat, for example released from heating or cooling of buildings, fossil burning and human metabolism contribute to the warming of the city (ibid.).

2.3.3 Effects on different scales

The effect of the urban fabric on energy partitioning has an effect on a micro scale but can also spread to affect a larger area. This depends on the different atmospheric layers created by the increased roughness of urban areas due to the changed surface (Gunawardena et al., 2017) acting on either meso or micro scale (Oke, 1976). At micro scale, in between urban roughness elements such as buildings, is the *Urban Canopy Layer* (UCL), influenced by the immediate surroundings and specific urban elements (ibid.). The UCL extends almost up to rooftop level in densely built areas but can completely lack at more open spaces (figure 1). The UCL also depends on wind strength, where influence from above lying air masses can penetrate through wind (ibid.). Above the UCL lies the *Urban Boundary layer* (UBL), which affects the city on a meso scale and is the air mass whose characteristics are modified by the presence of the city or urban area (Figure 1). Through these processes a phenomenon on a micro scale can have a far-stretched effect.

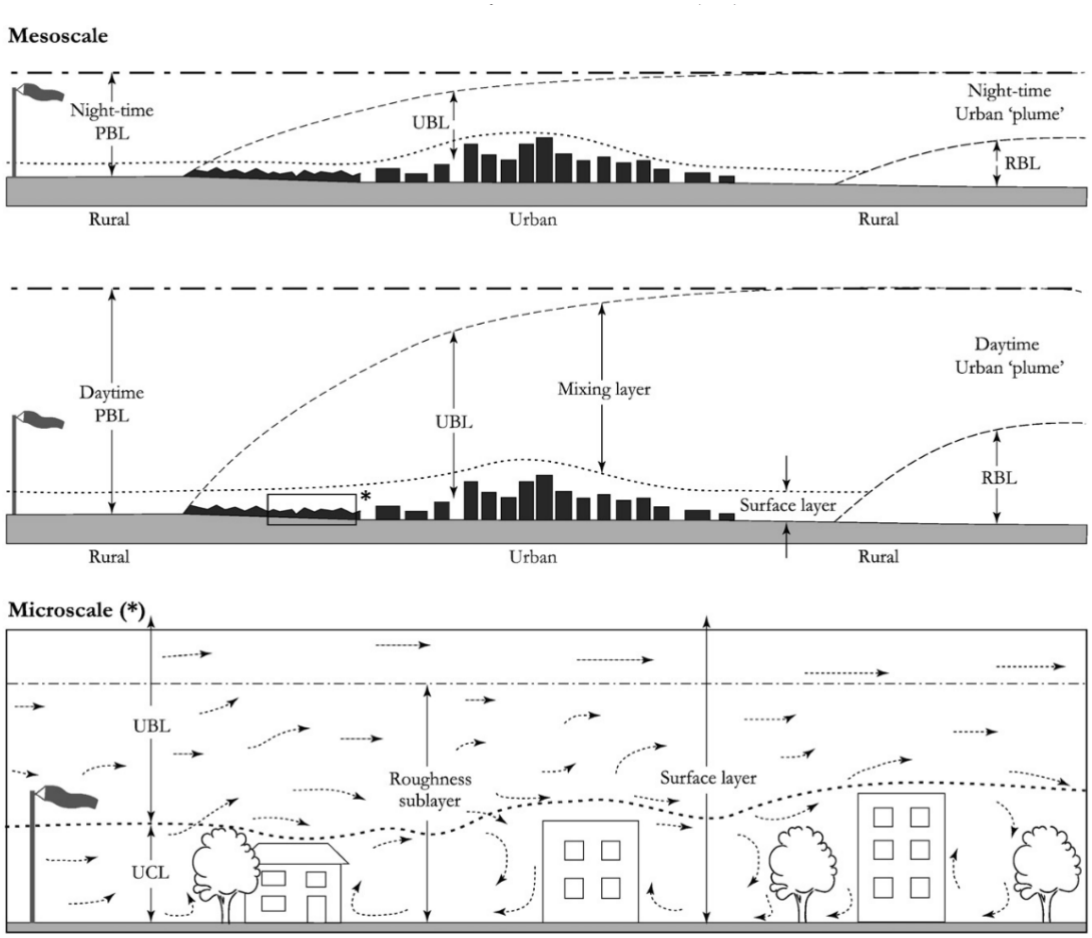

Figure 1. Atmospheric layers and the effect on different scales (Gunawardena et al., 2017 based on an illustration in Oke 1987)

2.4 BGI

There are many ways in which cities can take action against the effects of climate change and this section will describe measures that could affect the latent, and to some extent also the sensible heat flux.

2.4.1 Green roofs and rain gardens

In past planning of cities, grey infrastructure has been commonly used, meaning engineered structures to water management and climate adaptation, through solutions such as dams and pipes, which are not always the most cost efficient measure nor the most efficient in climate adaptation (Kabisch et al., 2017; Conservation International, n.d). In many cases blue-green infrastructure (BGI), also known as nature-based solutions, can be more efficient than grey infrastructure both in regards to costs and climate adaptation potential (Kabisch et al., 2017).

The definition of BGI is wide and there are different ideas of what should be included in the concepts. The European Commission states that BGI is "*a strategically planned network of natural and semi-natural areas (…) designed and managed to deliver a wide range of ecosystem services"* (European Commission, 2019). According to Simperler et al. (2020) the definition of BGI can be a natural blue and green area within the city, but also built systems using the natural potential of ecosystem services. Finewood et al. (2019) defines it as infrastructure that is intentionally designed to mimic and make use of the function of soils and vegetation. Even though the definition somewhat differs, research concludes that it involves greenery and water somehow for the purpose of minimizing consequences of climate change. It also concludes that BGI is valuable, for example regarding climate change adaptation, biodiversity, air quality enhancements and it also brings aesthetic value to the city (Kati & Jari, 2016;SMHI, 2019). BGI also benefits both physical and mental health among the inhabitants (World Health Organization, 2017; Kabisch et al., 2017) meaning that it is a multifunctional space in the urban environment that brings several benefits to the urban life. However, previous research upon BGI potential for cooling varies where streams, ponds and green roofs belong to the more researched fields (Sun & Chen, 2012; T. Sun et al., 2016). Rain gardens have been seen as an infrastructure that benefits runoff detention and not to have an effect on the reduction of urban temperatures, and research of this element is therefore scarce.

As stated above, BGI has several functions within the urban system where two of the most important for this thesis are related to the climate change adaptation strategies: water retaining capacity and potential to reduce heat stress (Simperler et al., 2020). Increased BGI and thereby increased permeable surfaces within the overall impervious environment of an urban area increases evapotranspiration, meaning the combined effect of evaporation of water from surfaces and transpiration of water from trees and plants (Kabisch et al., 2017). Through BGI, water is retained at the surface for a longer period of time, instead of going down into pipes, which increases the potential of evaporation from all types of surfaces, acting as a cooling agent for the environment (Carpener et al., 2017). The same BGI solutions are not universally applicable, as local characteristics affect the efficiency. For example, to maximize the benefit of evapotranspiration and thereby the effect of BGI, one should select native plants that are resistant to both wet and dry periods (Arabi et al., 2015).

2.4.2 Green roofs

Green roof is a broad term describing a roof on any type of building covered by a layer of vegetation (Capener et al., 2017). Green roofs are commonly divided into three types: extensive, semi-extensive and intensive roofs which describe the substrate depth, the plant species used and the need for maintenance (SMHI, 2019). Extensive green roofs have a thin substrate layer (30-150 mm) and are vegetated by plants such as sedum and succulent species (SMHI, 2019; Van Mechelen et al., 2015) (figure 2a). These species are superior to grasses and forbs when it comes to growing and surviving in dry conditions (Nagase & Dunnett, 2010). Sedum species can regulate and minimize transpiration during dry conditions, in order to preserve water and survive long periods without precipitation (Al-Busaidi, Yamamoto, Tanak & Moritani, 2013).

Semi-intensive roofs have a deeper substrate (120-350 mm) creating larger possibilities when deciding upon plant species, for example woody herbs, grass species and smaller bushes are suitable (SMHI, 2019; MacIvor & Lundholm, 2011). The intensive green roofs have a substrate layer thicker than 1 meter and require a sturdy construction due the weight of the structure, especially when wet (SMHI, 2019; Capener et al., 2017) (figure 2b.). All types of green roofs can have an impact on the local climate but to a different extent, where intensive roofs have the largest impact due to the large water holding capacity and the increased vegetation cover of large plant species (Capener et al., 2017). However, challenges also arise when installing a green roof, where one is to handle drought or dry periods (SMHI, 2019). Several factors, like the lack of moisture from ground water, the slope of the roof and exposure to wind, contribute to an increased drought risk for green roofs. This makes the tolerant extensive roofs a common choice. Since extensive roofs are easier to implement, the usage of this type of green roof is more widespread (Sun et al., 2016). Extensive green roof is also the type of roof implemented in Kvillebäcken and scenarios with this type of green roof will therefore be the focus of this study.

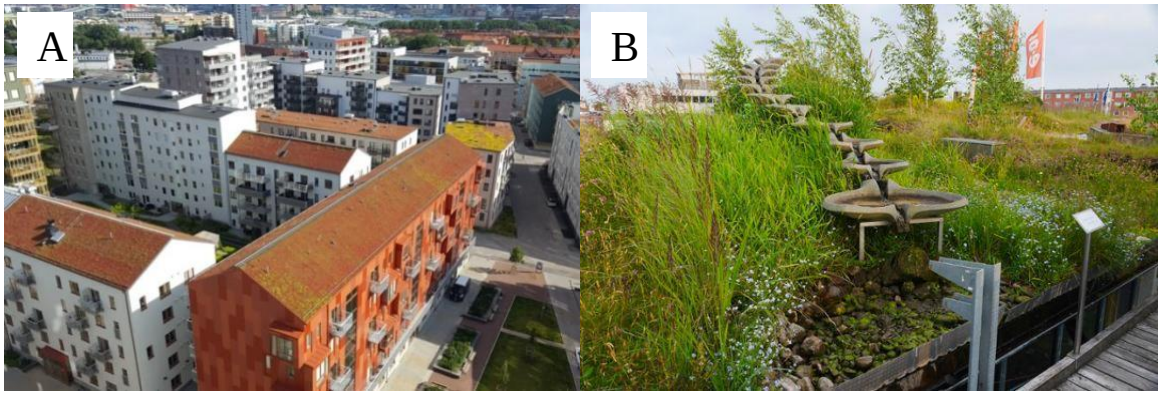

*Figure 2. Examples of **A**: an extensive roof during a dry period (Photo: Pär Johansson) and **B**: semi-intensive roof (Photo: Jonathan Malmberg).*

2.4.3 Rain gardens

A rain garden can be defined as a flower bed with high walls, where gutters lead runoff from buildings (Gothenburg municipality, n.d.). Rain gardens are mainly built to retain runoff in order to not overload the storm water system in urban areas (SMHI, 2018), but can also have a function of cleaning contaminated runoff before it enters the natural system (Venvik & Boogaard, 2020). Rain gardens also help restoring soil moisture and minimizing the effects of drought in periods with small amounts of precipitation (ibid.) As with green roofs, rain garden is a broad term, but can be defined as a structure normally consisting of "a sandy loam soil, a mulch layer and plants designed for retention, infiltration and treatment of storm water" (Muthanna, 2008). When incorporating pervious surfaces such as rain gardens into the urban structure, more soil water becomes available, which increases the latent heat flux and thereby possibly acts cooling for the surrounding air.

To maximize the function of rain gardens, it should be built with suitable plants, preferably native plant species that can grow in short periods of very moist soil, but more importantly that can withstand prolonged periods of drought (VA-guiden, 2020). Rain gardens in Kvillebäcken are defined as flower beds built with high walls where runoff water from roofs is led to it by drainpipes (figure 3).

Figure 3. One of the rain gardens in Kvillebäcken (Photo: Cornelia Wing)

2.4.4 High albedo roofs

High albedo roofs are an efficient climate adaptive strategy with the purpose to cool urban areas. These structures are sometimes also referred to as white roofs or cool roofs (Oke et al., 2017). High albedo roofs are roofs that have been painted or are covered in a light color. This is done in order to minimize the heat taken up and stored by buildings by using color that reflects a large part of the incoming radiation. This decreases the warming of the air mass above the roof. The high albedo roof is relatively cheap and easy to install and requires minimal maintenance (ibid.).

3. Study Area

3.1 The climate of Gothenburg

Gothenburg is the second largest city in Sweden in terms of inhabitants, being home to 583 056 people (SCB, 2020). The city is located on the west coast of Sweden (57° 42′ N, 11° 59′ E) and the climate is highly affected by the closeness to the Atlantic Ocean, giving Gothenburg a maritime climate (Oliver, 2005). The maritime climate affects the local weather on a day-to-day basis, giving relatively low summer temperatures (average 16.3 °C during June to August) and also mild winter temperatures (−0.4 °C in December to February) (Thorsson et al., 2017). Gothenburg receives about 670 millimeters precipitation per year, with the majority of it falling during fall and winter (SMHI, 2017). Precipitation is estimated to increase by 5-10% in the Gothenburg area until year 2100 (SMHI, n.d.).

3.2 Kvillebäcken

Kvillebäcken, the study area of this thesis, is located in the northern part of the city center (Gothenburg Municipality, 2021) (figure 5). Kvillebäcken is a mix of old and newer buildings and is mainly a residential area, but also hosts spaces for offices, restaurants, shops and other utilities (ibid). The study area in this thesis is limited to only the area known as Eastern Kvillebäcken (figure 5), which will further on in this thesis be referred to as Kvillebäcken. This area has been completely rebuilt during the last years.

The main goals when planning for this district was social and ecological sustainability, giving Kvillebäcken a modern feeling regarding architecture and urban structure (Gothenburg Municipality, 2020). The buildings in the area are in general four to six stories high and organized in an urban neighborhood structure where the ecological planning approach is visible through greenery incorporation in patios, on roofs and in the park surrounding the stream passing through the area (ibid.). The new parts of Kvillebäcken differ a lot from the surrounding areas regarding building structure (figure 4).

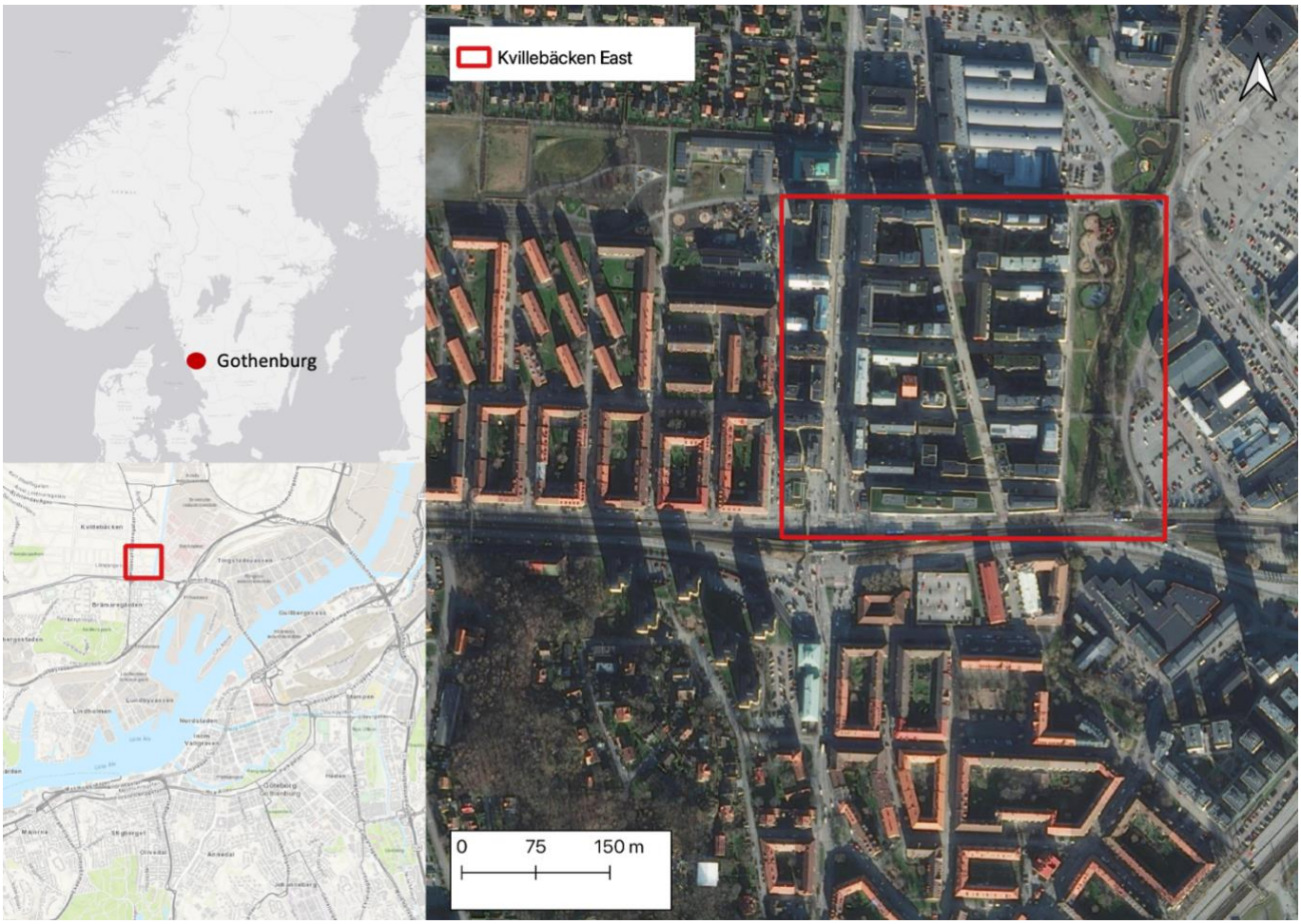

Figure 4. Map illustrating the study area of Kvillebäcken, where it is located within the city of Gothenburg and within Sweden. The satellite image also displays the differences in structure between the newer and the older parts of the neighborhood.

4. Materials and Methods

The following section describes data processing and methods used for this thesis. Modelling requires extensive pre-processing specific to each dataset, which will be presented below in categories based on processing technique and data type.

4.1 Description of model

Urban areas are continuously growing, and in order to understand how to create resilience for cities in a changing climate it is necessary to understand how the urban structure and the materials affect the urban energy balance at different scales (Best & Grimmond, 2015; T. Sun & Grimmond, 2019). Climate modelling is necessary to obtain information on how different measures have potential to reduce urban heat stress (ibid). Urban Land surface models are commonly used to model water and energy fluxes in urban areas (Sun & Grimmond, 2019). The specific model used in this thesis is The Surface Urban Energy and Water balance Scheme (SUEWS), which simulates both energy and water fluxes in urban areas (Ward et al., 2016) based on meteorological data, ground cover and a vector grid defining the area of interest (SUEWS Manual A, 2019). The model is able to simulate energy and water fluxes in cold climate cities (Järvi et al., 2014) which makes it suitable for modelling the Gothenburg area. The basics of SUEWS is the urban energy balance (Oke, et al., 2017) and the urban water balance (Ward et al., 2016). The output from the model is several types of energy fluxes as well as parameters related to water, such as precipitation, runoff and water storage (figure 5).

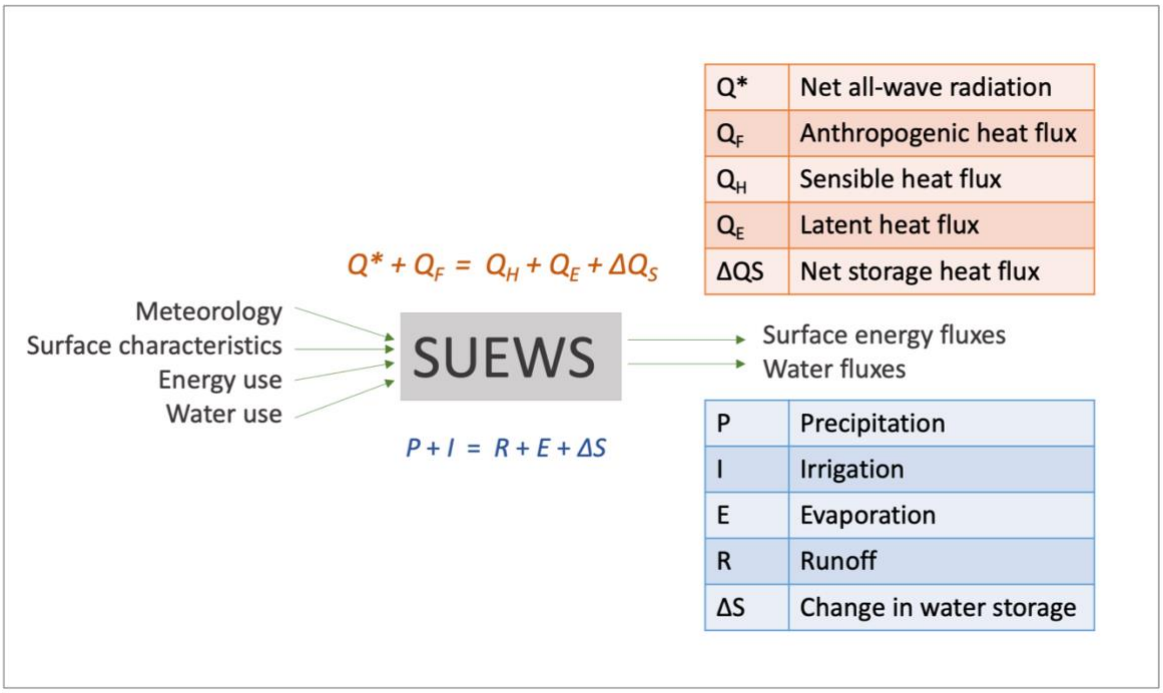

Figure 5. Input and output from SUEWS. Based on image from SUEWS Manual A (2019).

4.1.1 SuPy

SuPy (a version of SUEWS handled through Python) was used in this thesis due to easier handling and overview of the model, input parameters and runs. SuPys' scientific thoroughness is guaranteed by SUEWS (ibid) and has been developed because of the increasing knowledge in Python among climate researchers, where SuPy has expanded the usability of SUEWS. Further information on how SuPy works can be found in Sun & Grimmond (2019). SuPy version 2021.3.30 was used in this thesis, which at the time was the most up to date version. The model running period was 2017-2018 with hourly resolution, where 2017 was used as a spin-up year in order for the model to stabilize (T. Sun & Grimmond, 2019) and 2018 was the year which was used to interpret results. Further in this thesis, SUEWS will be used as the name of the model except when dealing specifically with calculations and other settings that have been done outside SUEWS. In these cases, the name SuPy will be used.

4.2 Data and data processing

4.2.1 Meteorological data

The meteorological data set, retrieved from the Swedish Meteorological and Hydrological Institute (SMHI) from the station Gothenburg A, was processed in order to fit the format of SUEWS. For this thesis work, the SUEWS minimum requirement regarding meteorological variables as input data have been used (table 1).

The data was downloaded separately for each parameter (SMHI n.d.). The files were merged into a text file covering all parameters on an hourly resolution. Missing data was interpolated through a linear interpolation method (Pandas Manual, 2021) up to a maximum of 5 hours in the event of missing data.

Table 1. Required meteorological input data in SUEWS (UMEP Manual B, 2020)

Variables
Wind speed (m/s)
Air temperature (°C)
Relative Humidity (%)
Barometric pressure (kPa)
Incoming shortwave radiation [W m-2]
Precipitation(mm)

4.2.2 Elevation Models

Terrain models were used in order to obtain topographic attributes, building and vegetation heights of the study area (See Reddy, 2018). All three elevation models in this thesis are retrieved by LiDAR measurements and have then been converted into raster files of a resolution of 1 meter. Three different elevation models were used, Digital Elevation Model (DEM) which is a representation of the ground surface elevation, Canopy Digital Surface Model to obtain the height of vegetation within the city and the Digital Surface Model (DSM) showing the height of objects in relation to the ground elevation.

Kvillebäcken is an area of development and new buildings have been added since the DSM was first created and it had to be updated in order to represent the area today. Then the height of the buildings was measured using a Nikon Laser Forestry Pro. This tool measures angles

and horizontal distances, allowing for easy height measurements at the building site (Nikon, n.d.). Every building was measured three times and an average of these three measurements were calculated. However, due to the dense building pattern there were some issues of measuring the highest point of the roof of those buildings having a gable roof (about 1/3 of the buildings). Instead, all buildings were measured where the lower part of the roof meets the wall, to have equal measurements on all buildings.

Further pre-processing of the data was necessary in order to obtain morphometric parameters later used in SUEWS, such as building height, plan area index and vegetation height. The land cover data was processed in a similar way to retrieve the fraction of every land cover type for the chosen area (table 2).

4.2.3 Land cover data

The land cover data used is an updated version of the land cover raster created by Johansson (2017) and it uses seven different classes (table 2) (SUEWS Manual A, 2019). Due to the rebuilding of Kvillebäcken during the last years the land cover had to be updated, where the separate land cover classes were retrieved differently.

Table 2. Land cover types in land cover layer and the corresponding fraction in the Kvillebäcken Base Scenario.

Land cover type	**Fraction of each land cover**
Paved	0.445
Building	0.319
Evergreen tree	0
Deciduous tree	0.041
Grass	0.162
Bare ground	0.012
Water	0.021

Evergreen trees were removed from the land cover since there are only a few of those in the whole research area and their impact is seen as negligible. Deciduous trees were added to the land cover layer based on a digitalization of vegetation in Kvillebäcken made by Wing (2021). Grass and other vegetation elements such as green roofs and raingardens were also taken from this source (ibid.). Buildings were added into the land cover layer using the difference between

the DSM and the DEM layer. Water, which only is present in the stream that runs through the area, was used from the unaltered land cover data set since the stream has kept its original shape during the rebuild of the area. Bare soil was manually added and is only present at a few walking paths and similar features. Lastly, paved was retrieved as a residual, by filling all empty areas not covered by another land cover class.

4.2.4 Population

Kvillebäcken is mainly a residential area and therefore the population is estimated to peak at nighttime when people are home from daytime occupation. Data from the statistical analysis department of the City Executive Office of Gothenburg was used to identify daytime and nighttime populations, where the Kvillebäcken population more than tripled at nighttime which affects the anthropogenic heat flux (Table 3).

Table 3: Estimated daytime and nighttime population in Kvillebäcken per hectare.

Population Daytime / ha	**Population Nighttime / ha**
82.5	295.3

4.3 Creating Scenarios

In order to model the effect of a larger share of rain gardens and green roofs, scenarios for the different BGIs had to be set. The first scenario is referred to as the Base Scenario (table 4) and is the best possible representation of Kvillebäcken, but without any BGI other than the grass following the land cover settings. Important to note is that two types of BGI are modelled separately, meaning that when investigating building runoff to rain gardens and grass areas, this is done assuming that there are no green roofs in Kvillebäcken.

Table 4. Parameter settings for the Base Scenario (See Suews Manual B, 2019).

Parameter	**Setting**
Albedo	0.15
Emissivity	0.91
Water storage	0.25 mm
Wet threshold	0.25 mm
State Limit	0.25 mm

For example, regarding albedo and emissivity on roof material and soil aspects looking at rain gardens. To investigate scenarios where areas to a larger or smaller extent are covered by either of the two types of BGI investigated in this thesis, the scenarios were put to describe the effect of 100% coverage of either green roofs or rain gardens. For lower scenarios, such as 25% coverage, 50% coverage or 75% coverage a weighted average was used. For example, when looking at a coverage of 75% green roofs (out of the total roof area), 75% of the output of a SuPy run is taken from the scenario of 100% green roofs and 25% of the result is taken from the Base scenario (figure 6).

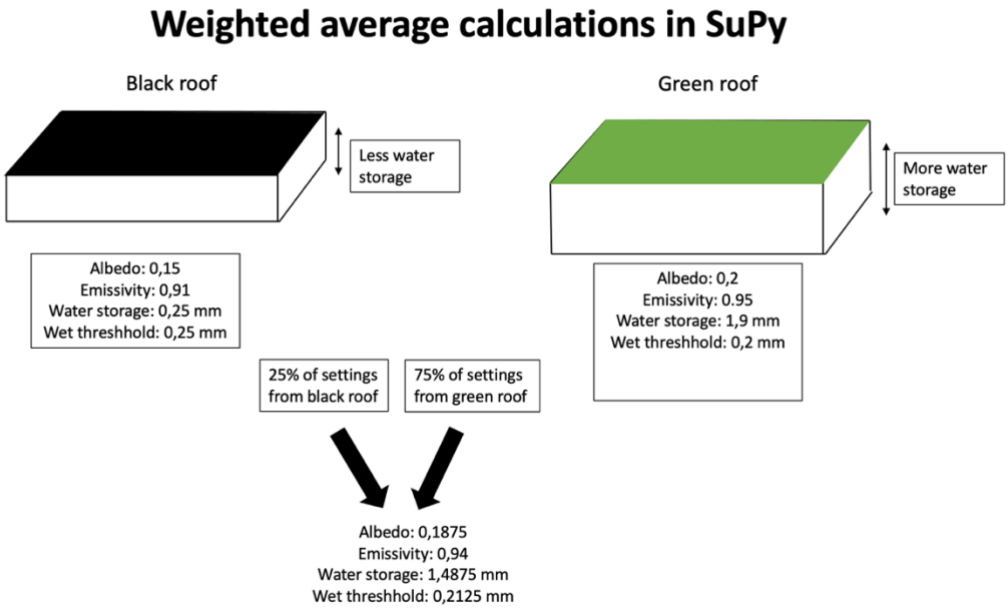

Figure 6. Illustration of how weighted average was calculated (example showing 75% green roof) after a run in SuPy. The same method was used for all scenarios of different amounts of green roof coverage was calculated.

4.3.1 Green Roofs

Settings to model extensive green roofs mainly relate to the albedo, emissivity and water storage capacity of green roofs. This means that the model shows what effect a green roof has on the energy partitioning in urban areas, when changing surface and water storing factors from a more standard roof into a representation of a green roof (Table 5).

Table 5. Parameter settings for a green roof (Suews Manual B, 2019).

Parameter	**Setting**
Albedo	0.2
Emissivity	0.95
Water storage	1.9 mm
Wet threshold	2 mm
State Limit	1.9 mm

This method to model green roofs does not account for the cooling effect of transpiration from plants in the way an actual green roof is assumed to function. The modelled green roof has a higher capacity to store water compared to ordinary roofs, which increases the potential evaporative cooling. This way of modelling green roofs does not represent the exact effect an actual green roof would give but since the evapotranspiration tend to be low or negligible from extensive green roofs in arid conditions, it can still be argued to give an idea of how these installations affect the energy partitioning (Van Mechelen et al., 2015). In order to have a comparison and set the effect of green roofs into a context, the effect of a high albedo white roof has also been investigated.

4.3.2 Rain gardens

Since rain gardens are constructed at ground level, these were modeled as grass but with parameters changed into a more suitable way for how rain gardens are built in regard to soil type, soil depth and type of vegetation. Albedo, emissivity and soil characteristics were changed in order to achieve a modeled rain garden (Table 6.). Further, an increased share of runoff from building roofs were also led to these rain gardens in order to investigate how increased water availability in this type of BGI can potentially increase the latent heat flux.

Table 6. Parameter settings for a rain garden (Suews Manual C, 2019).

Parameter	**Setting**
Albedo	0.18
Emissivity	0.94
Water storage	2.3 mm
Wet threshold	1.8 mm
State Limit	1.9 mm

4.3.3 Scenarios for increased BGI and high albedo roofs

The present BGI in Kvillebäcken differs between the two types, where quite a large proportion of the roof area is already covered by green roofs but only 3% of the total ground vegetation is made up by rain gardens. The two also differ in the space they take up in the urban environment, where rain gardens compete with all other interests on ground level while the roof area isn't commonly competing with other interests. Therefore, they have been set to different scenarios that can be assumed to be reasonable for the two types of BGI (table 8).

Since there already is quite a large share of green roofs in Kvillebäcken, one can assume that increasing these would be possible since most of the roof area that is not used for green roofs today is not used for any other purpose either. It can also be argued that if a similar area was to be built, which is likely according to the city's plans for densification (Gothenburg Municipality, 2020) a larger proportion of green roofs is feasible. Due to this, the scenarios for increased green roofs have been set to 50%, 75% and 100% of roof area covered by green roofs (table 8). In order to compare the effects of installing green roofs, a high albedo roof has also been modelled. The high albedo roof is shown in a 100% scenario and can be compared to the effects of the 100% scenario of green roofs (table 7).

Table 7. Parameter settings for a high albedo roof (Suews Manual B, 2019).

Parameter	**Setting**
Albedo	0.6
Emissivity	0.95
Water storage	0.25 mm
Wet threshold	0.25 mm
State Limit	0.25 mm

For rain gardens, scenarios have been set lower since rain gardens today only make up a small part of the vegetation cover, which means that it is not reasonable that one would see 50% or 75% of the ground vegetation cover being rain gardens. Therefore, scenarios have been set based on possible changes to current flowerbeds in Kvillebäcken. If all flowerbeds are included into vegetation cover, they, together with raingardens make up about 30% of the total ground vegetation in Kvillebäcken. It would be a large project, but through increasing the height of the flowerbed walls and lead precipitation runoff there, they would become rain gardens (table 8).

4.3.4 Scenarios of changed land cover and increased water to BGI

In Kvillebäcken today, about 10% of runoff from buildings is led to vegetation. In order to investigate how runoff from buildings can increase the latent heat flux from rain gardens, the model was also run with 100% of the runoff from buildings being led to each of the rain gardens scenarios. Further, to be able to compare the potential of rain gardens, scenarios of increased fractions of grass areas in Kvillebäcken were used to investigate whether only grass also has an effect on the latent heat flux. The fraction of grass in Kvillebäcken today is approximately 16% of the total area. Scenarios used when increasing the grass area was 26% grass, 36% grass and 46 % grass out of the total area. For these scenarios to be created, it was necessary to decrease other areas. This was done by reducing the area covered by paved surfaces by the corresponding amount for each scenario. However, to increase the fraction of grass according to these scenarios is not a probable action in Kvillebäcken. It is however useful to look at in order to evaluate the effect of grass on latent heat and thereby possibly suggest a higher fraction of grass if more areas are built/rebuilt in the same style as Kvillebäcken. To investigate further what influence grass can have on the latent heat flux, more precipitation runoff from buildings were also led to grass areas. The three scenarios for grass were used, and 100% of building water was led to each to demonstrate the difference with more available water.

Table 8: List of scenarios and the corresponding short name used in plots.

Scenario short name	Scenario full name	Comment
base	Base Scenario	0% rain gardens and 0% green roofs
rg_30	30 % rain garden	% rain gardens of all vegetation
rg_10	10 % rain garden	% rain gardens of all vegetation
rg_3	3 % rain garden	% rain gardens of all vegetation
rg_30_water	30% rain garden plus water	100% of building runoff led to 30% rain garden coverage
rg_10_water	10% rain garden plus water	100% of building runoff led to 10% rain garden coverage
rg_3_water	3% rain garden plus water	100% of building runoff led to 3% rain garden coverage
gr_100	100% green roof	100% green roof coverage
gr_75	75% green roof	75% green roof coverage
gr_50	50% green roof	50% green roof coverage
gr_25	25% green roof	Green roof coverage today in Kvillebäcken
gr_white	100% high albedo roof	100% high albedo roof coverage
grass_26	26% of land cover is grass	Land cover fraction grass increased to 0.26
grass_36	36% of land cover is grass	Land cover fraction grass increased to 0.36
grass_46	46% of land cover is grass	Land cover fraction grass increased to 0.46
grass_26_water	26% of land cover is grass plus water	Building runoff led to 0.26 grass fraction
grass_36_water	36% of land cover is grass plus water	Building runoff led to 0.36 grass fraction
grass_46_water	46% of land cover is grass plus water	Building runoff led to 0.46 grass fraction

4.3.5 Case study periods

The meteorological periods were chosen based upon the amount of precipitation and time in between rain events. The dry period (2018-07-16 to 2018-07-23) is a part of a heatwave with an extended period of unusually hot temperature for Gothenburg together with a low amount of precipitation during the summer of 2018 (figure 7A). The wet period is from the same year, but in October (2018-10-02 to 2018-10-08) when precipitation was more frequent (figure 7B). The case study periods were chosen to show a week at two specific time periods during 2018 since it can show a detailed pattern on a short time scale such as 24 hours. However, it also displays the time it takes for the effect of a rainfall to disappear.

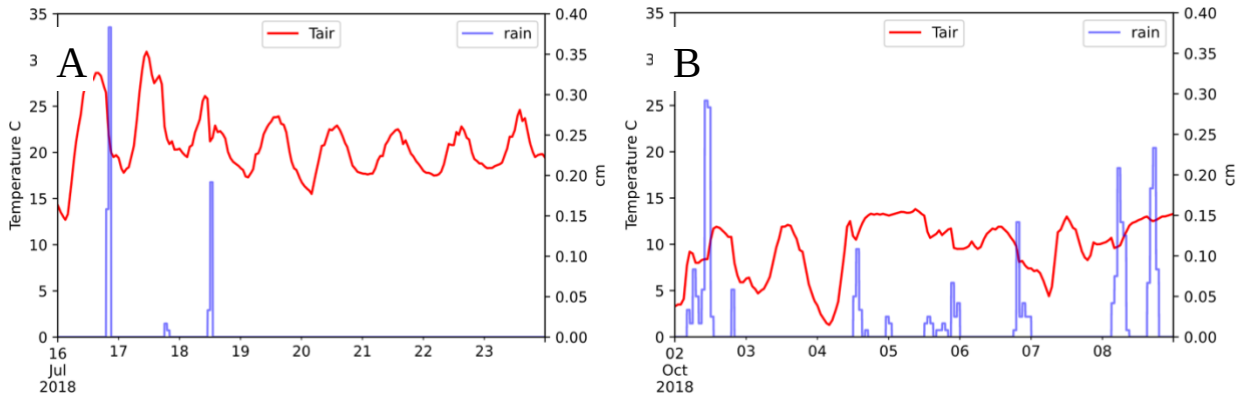

*Figure 7. The meteorological periods selected for this thesis work, where **A** illustrates the dry period and **B** represent the wet period.*

5. Results

This section presents the results from running SuPy with the different scenarios. It displays the energy partitioning in Kvillebäcken with the current extent of rain gardens and green roofs, and how changes regarding these structures can have an effect, mainly on the Q_E energy flux but also to a certain extent on the Q_H energy flux. Plots are presented either as the latent heat flux (Q_E) or the sensible heat flux (Q_H) divided by the Available Energy (AE), giving the fraction of Q_E or Q_H in relation to AE or as watts per square meter (Wm^-1).

5.1 Overview of Model run

The model run for 2018 (figure 8) displays the changes in the Surface Energy Balance over the year, where the incoming net radiation (Q*) and sensible heat (Q_H) peaks during June and July, whereas the latent heat (Q_E) reaches the highest values later during the year, during August and September. The Surface Water Balance displays the unusually dry spring and summer with little precipitation (figure 11). Evaporation and latent heat increase during August when precipitation is increasing.

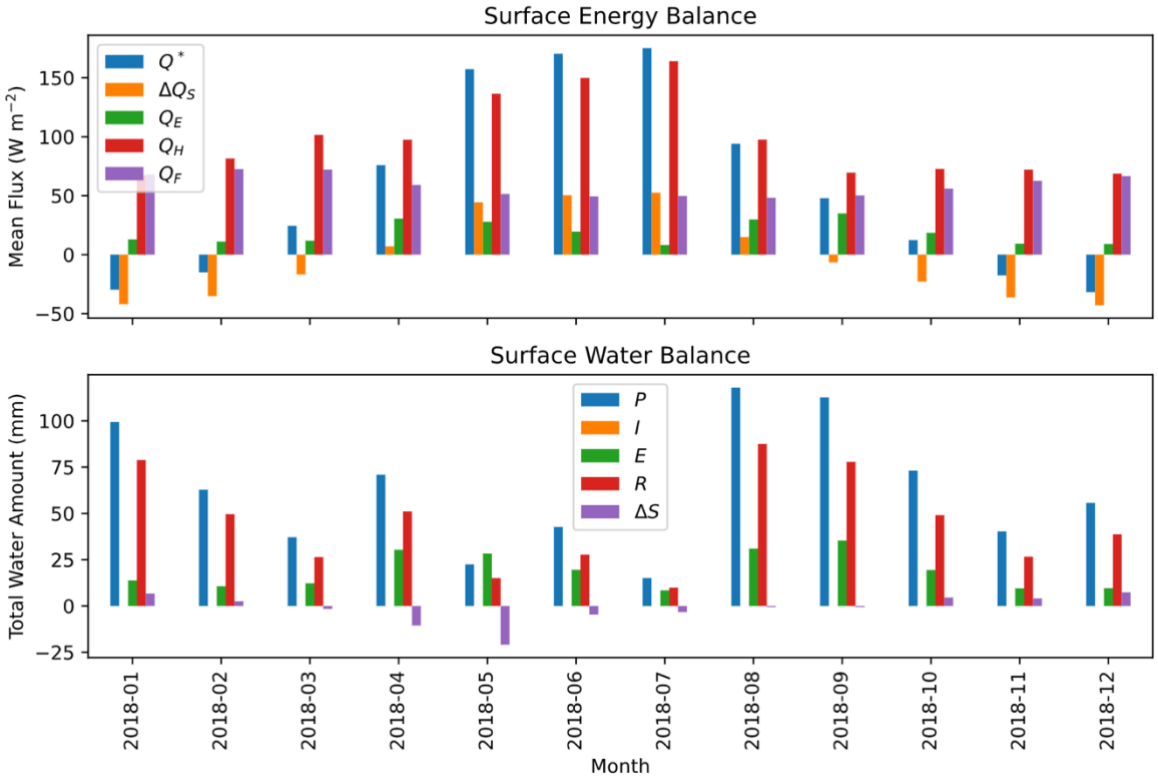

Figure 8: Model output showing Surface energy balance and Surface water balance of 2018 presented as monthly average for each flux.

5. 2 The energy partitioning of Kvillebäcken

5.1.1 Rain Gardens

Q_E reaches the peak value as a direct effect of a rainfall event, which has a decreasing influence on the Q_E fraction during up to 24 hours. The difference between the Base scenario and 3% rain garden is only at its largest barely 1% (0,01), meaning that the current extent of rain gardens in Kvillebäcken has little influence on the latent heat flux (figure 9b).

The effect of an increased area of rain gardens in relation to other vegetation, there is for the dry period an evident effect of rainfall on the partitioning of Q_E. The effect disappears quickly, within 24 hours of the rain event. Without precipitation, the rain gardens do not have an effect on the Q_E fraction. For scenarios with 10% rain gardens and 30% rain gardens, the rise in Q_E is larger but does not last for a longer period of time (figure 9b). For the wet period, the fraction of Q_E is more constant due to more frequent precipitation events. However, the difference from the Base scenario is smaller which likely is an effect of the cooler temperatures during this period, giving a smaller rate of evaporation (figure 10).

When looking at an increased fraction of rain gardens and how an increased amount of runoff from buildings affects the Q_E, it is evident that the Q_E fraction becomes larger when more water is led from buildings. The effect over time is however small and the difference in the rise of Q_E from the Base scenario remains less than 24 hours for all rain garden scenarios (figure 9b).

The wet period follows the same pattern as the dry period, showing that rain gardens with 100% of building runoff increases the fraction of Q_E directly after a rainfall event but the effect is only short-term (figure 10). However, when comparing the different rain garden scenarios, it should be noted that these results show that a smaller amount of rain gardens but with a large amount of water led to it (ex. 10% rain garden with added water, red line) increases Q_E flux more than 30 % rain garden (purple line) directly after a rainfall event (figure 10b) during the wet periods. However, the relationship is the opposite a few hours after a rain event, where the scenario 30% rain garden contributes to a larger fraction of Q_E (figure 10b).

During the wet period Q_E levels are similar to the dry period values. However, due to more consistent rainfall events the Q_E fraction is slightly higher than the base scenario for most days. This is in contrast to the dry period where Q_E levels remain the same for Base and 3% rain gardens within 24 hours after the last rain event (Figure 10b).

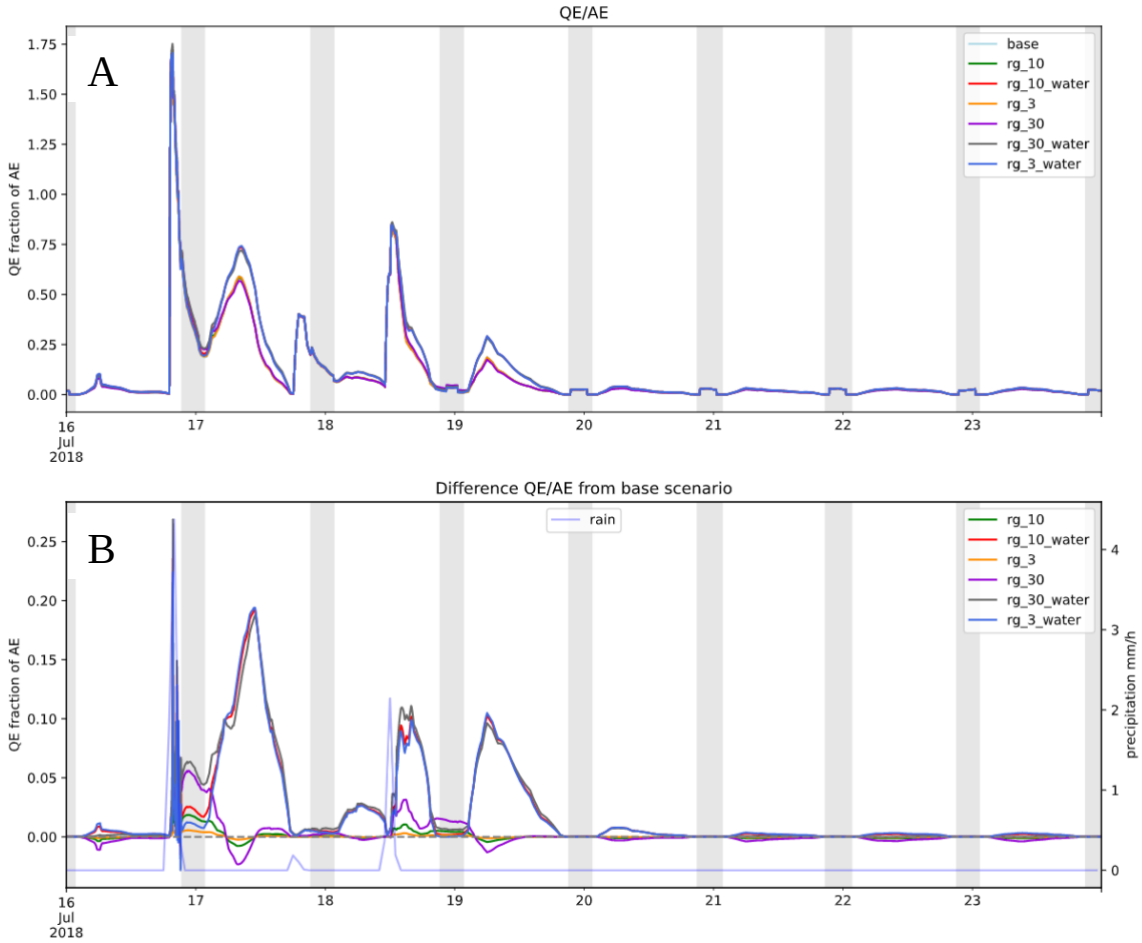

Figure 9. The effect of an increased surface area of rain gardens in the dry period, and also 100% of building runoff led to each scenario. ***A****: Fraction of* Q_E *and* ***B****: difference from the base scenario.*

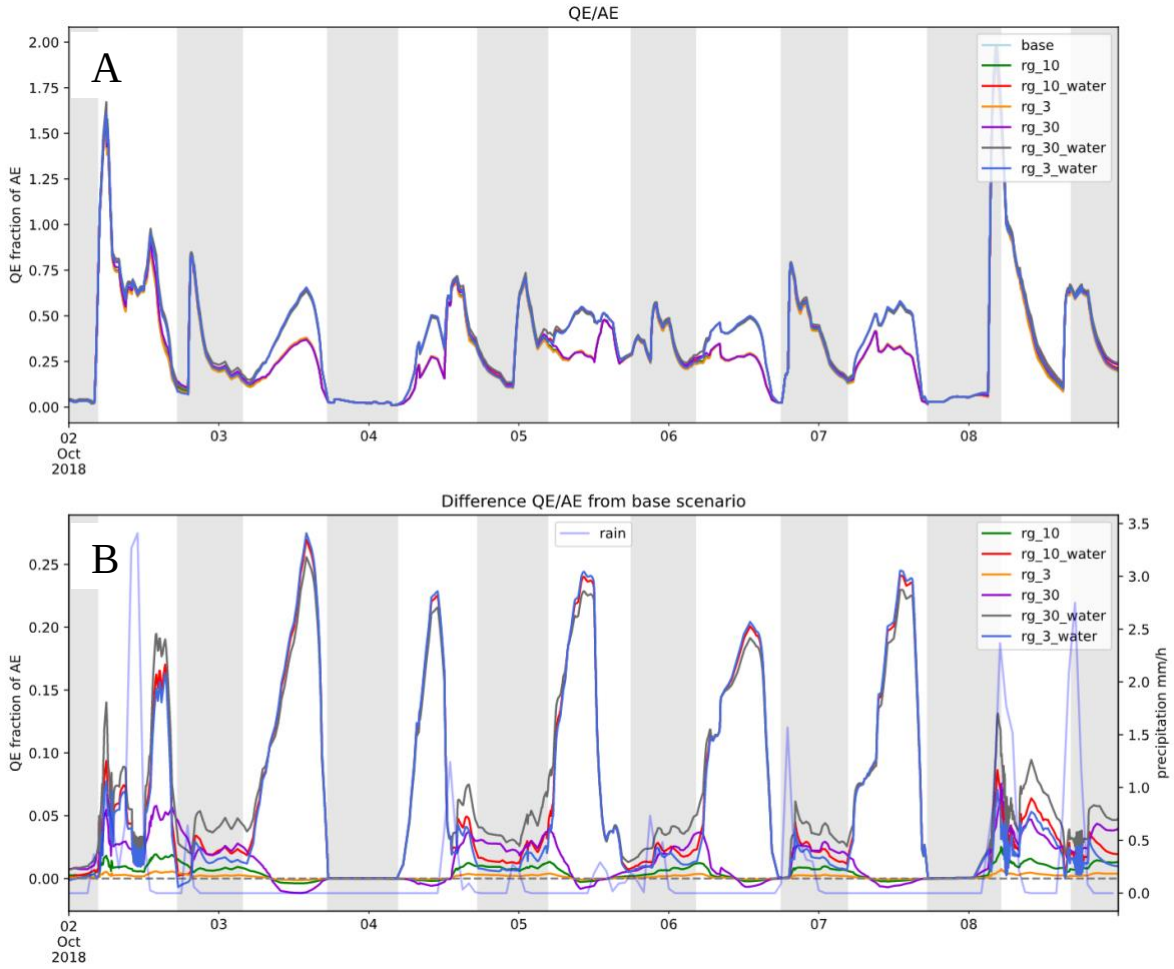

Figure 10. The effect on Q_E fraction when the surface area of rain gardens is increased, in the wet period and 100% of building runoff led to each scenario. ***A****: Fraction of Q_E and* ***B****: difference from the base scenario.*

5.2.2 Green roofs

The Q_E fraction is higher for the 25% scenario than the Base scenario during rain events and the effect lasts up to 24 hours, where the effect depends on the magnitude of the rain (Figure 11 & 12). There is no rise of Q_E on days without rainfall (Figure 11b) during the dry period, demonstrating that green roofs do not increase evaporative cooling on days without precipitation in Kvillebäcken with current green roof coverage. For the wet period (figure 12), the pattern is similar to the dry period, but the effect of an increased Q_E fraction lasts slightly longer. The fraction of Q_E is more constant during the wet periods but is also an overall smaller fraction of AE, likely due to the lower temperatures of this period compared to the dry period, which decreases the evaporation possibilities for surface water.

During the dry period there is an effect on the Q_E fraction after rainfall events, which is clearly increasing for each scenario of green roof coverage (figure 11 & 12). The effect is large directly after a rain event but decreases rapidly during the following 24 hours and ceases after that. During days of no precipitation there is no effect for any scenario on the Q_E fraction from green roofs. The Q_E increasing effect lasts the same period of time for all scenarios (figure 11 & 12).

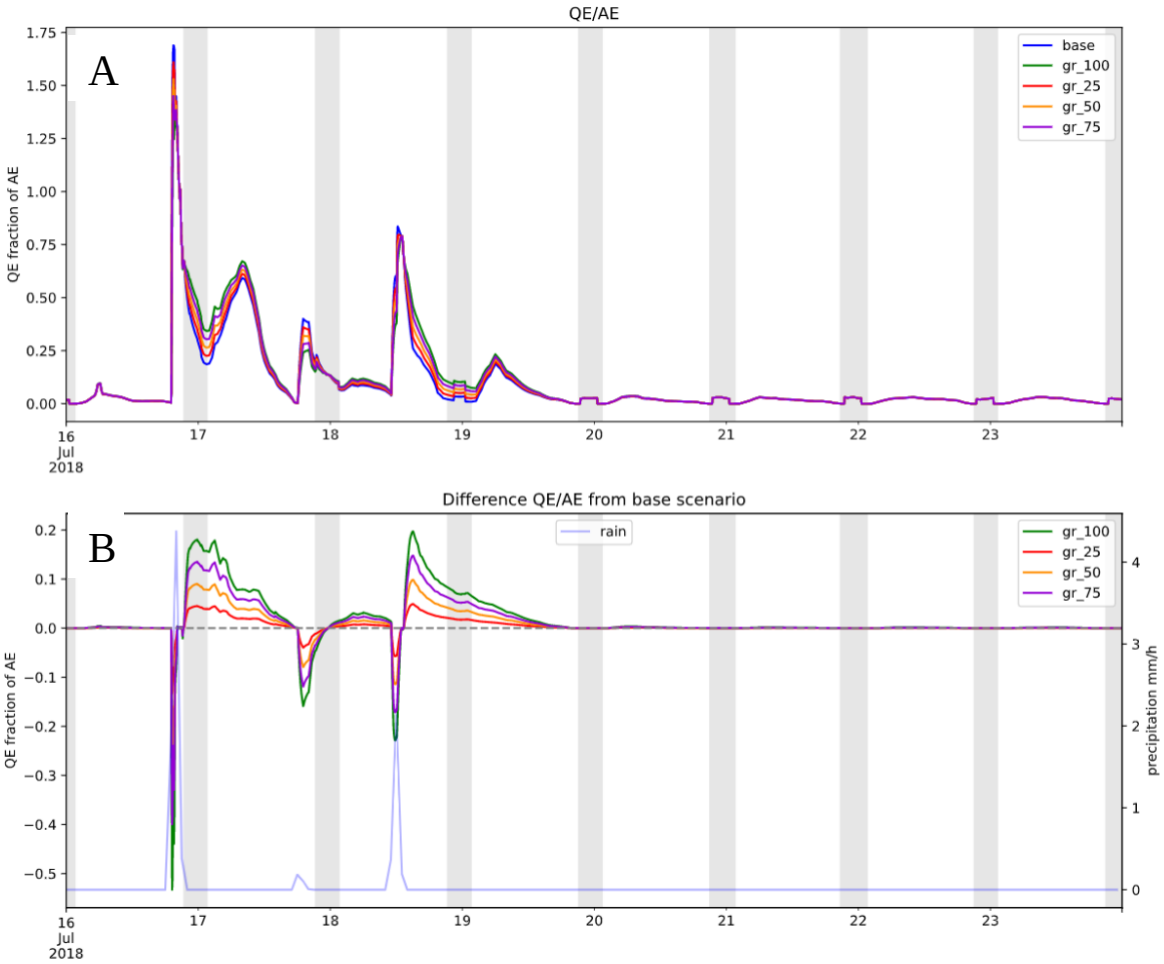

Figure 11. Effect on Q_E using green roof scenarios during the dry period, modelling present green roof cover (25%) and increased scenarios of 50%, 75% and 100% coverage for the dry period. ***A:*** *Fraction of Q_E for each scenario and* ***B****: difference of each scenario from the base scenario.*

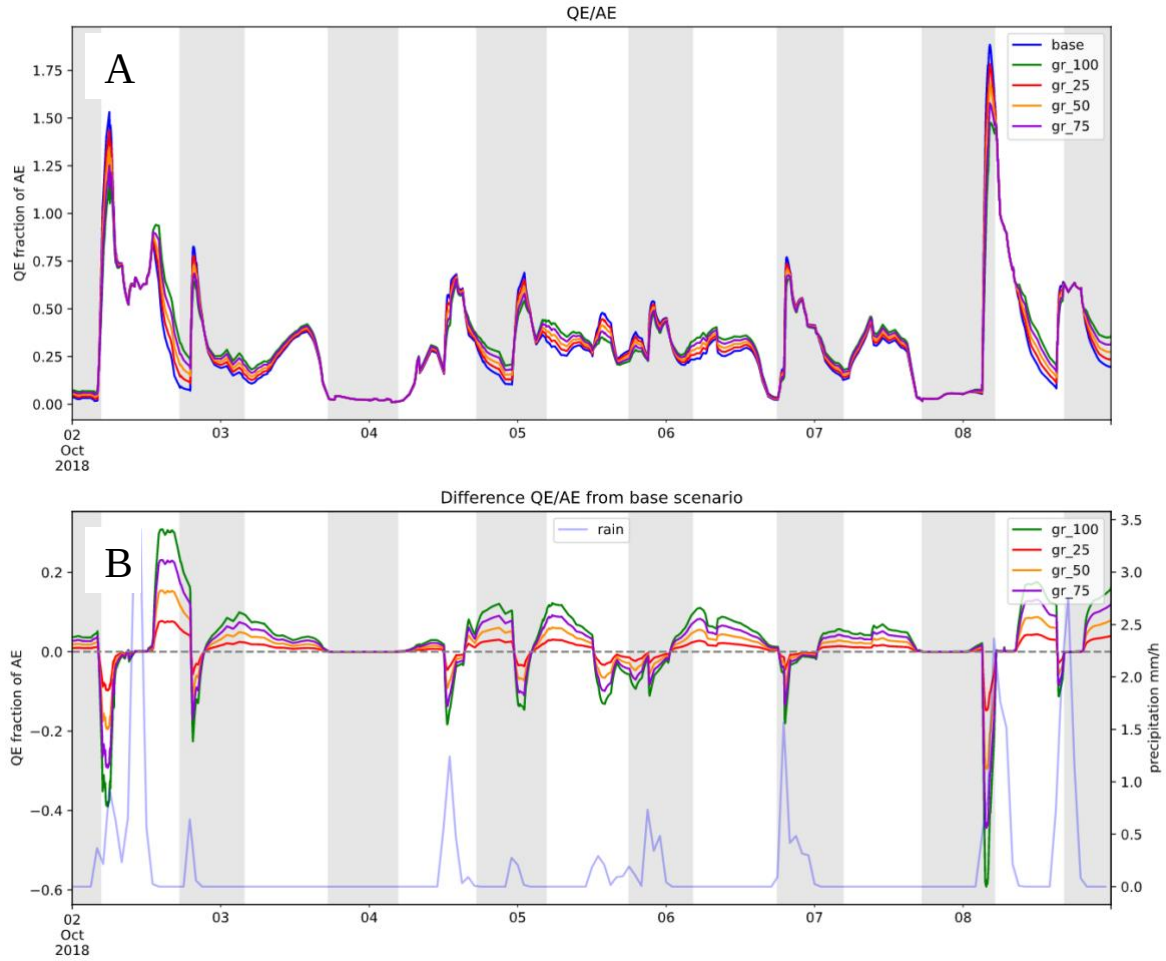

Figure 12. Effect on Q_E using green roof scenarios during the wet period, modelling present green roof cover (25%) and increased scenarios of 50%, 75% and 100% coverage for the wet period. ***A:*** *Fraction of Q_E for each scenario and* ***B****: difference of each scenario from the base scenario.*

5.2.3 Increased grass land cover fraction

An increasing fraction of grass gives a clear increase in fraction of Q_E, and when building runoff is led to grass, it increases the fraction of Q_E further. The increased Q_E lasts about 24 hours during the dry period (figure 13) and a little longer during the wet period (figure 14). Overall, during the wet period the pattern is similar where an increased amount of water led to all three scenarios increasing the Q_E fraction (figure 13 & 14). The Q_E fraction is kept at a higher overall level during the wet periods with frequent rain events (figure 14).

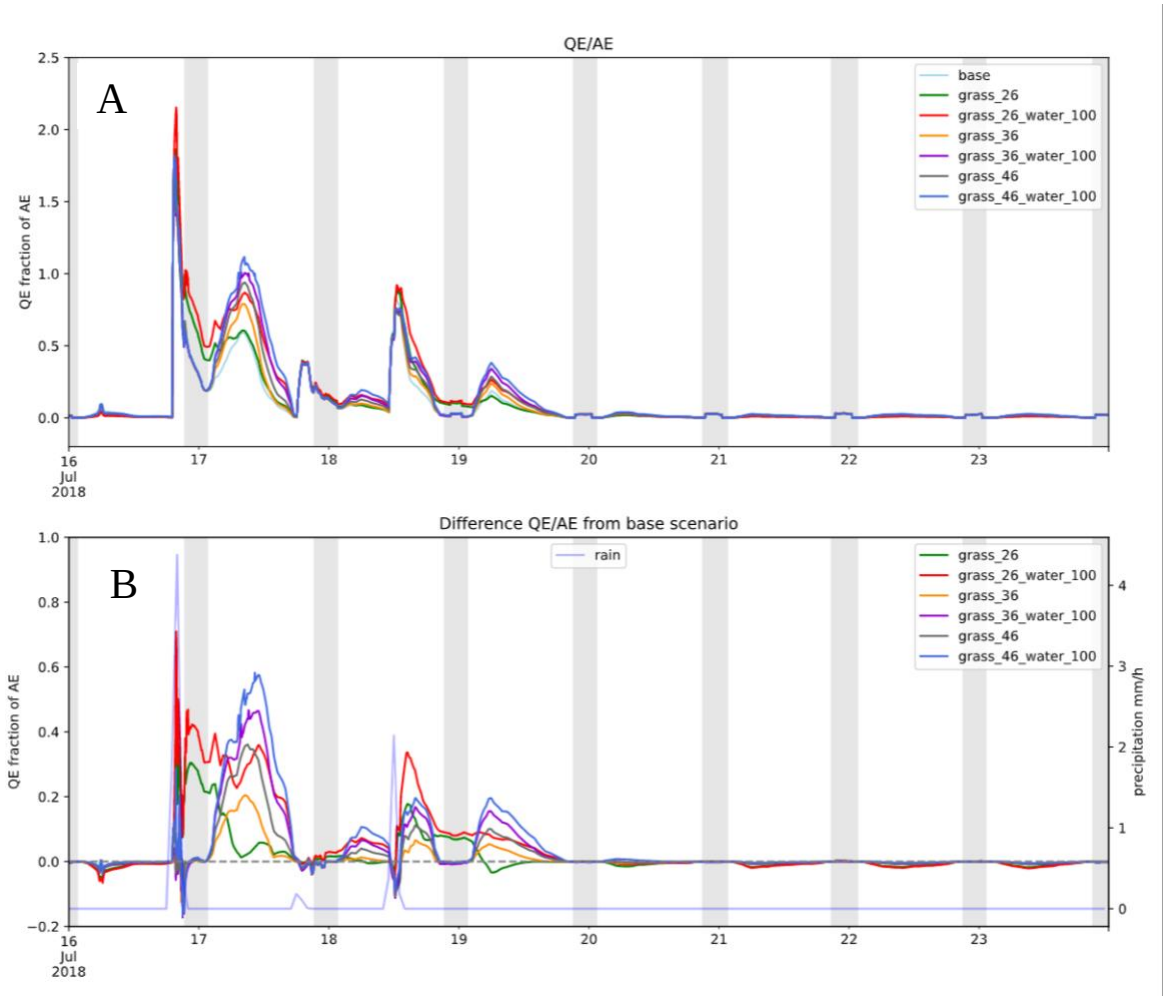

*Figure 13. Different scenarios of grass fractions in Kvillebäcken and how the Q_E fraction changes when leading 100% of building runoff to these grass areas during the dry season. **A**: Fraction of Q_E with different grass fraction scenarios. **B**: Difference from each scenario to the base scenario (16% grass coverage).*

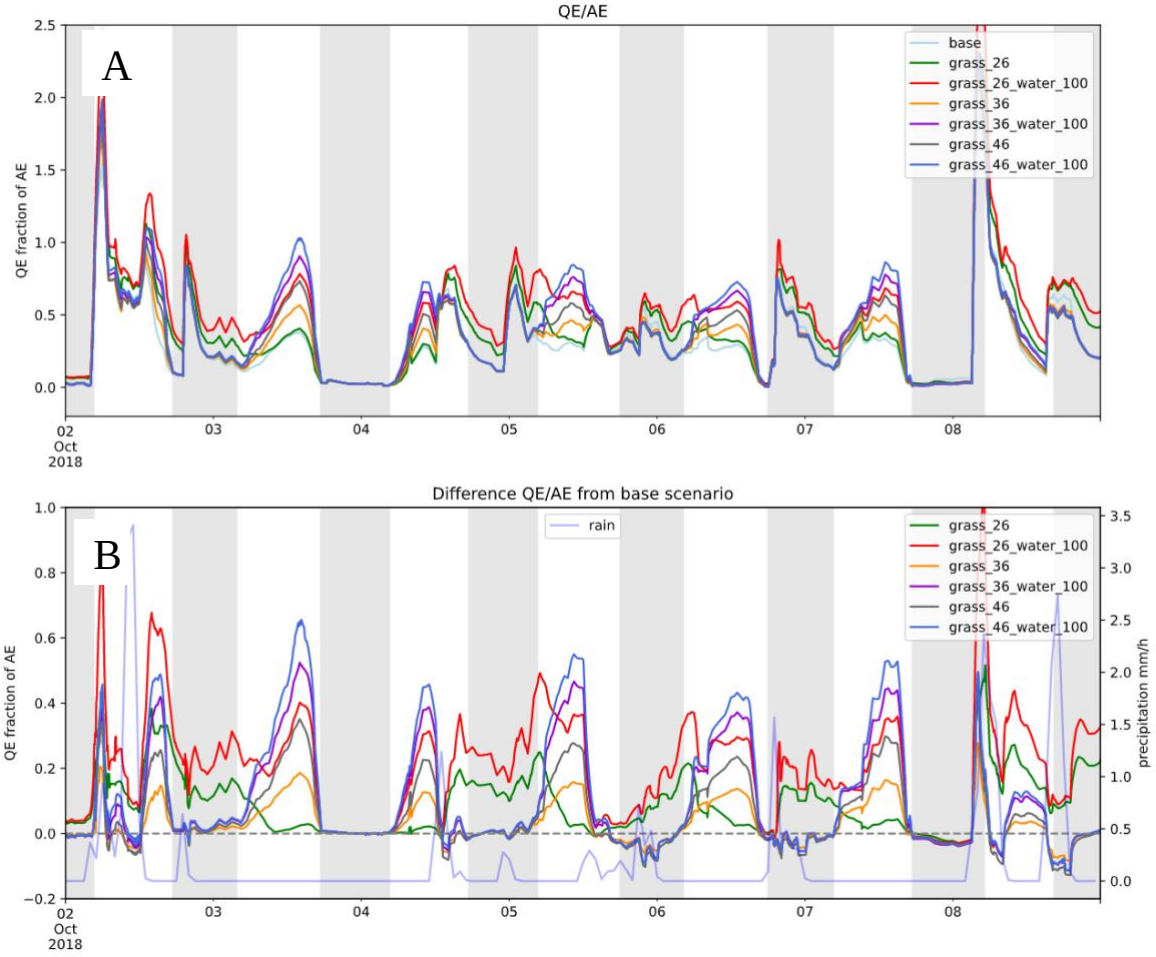

Figure 14. Different scenarios of grass fractions in Kvillebäcken and how the Q_E fraction changes when leading 100% of building runoff to these grass areas during the wet season. ***A****: Fraction of Q_E with different grass fraction scenarios.* ***B****: Difference from each scenario to the base scenario (16% grass coverage).*

5.2.4 The effect of green and high albedo roofs compared

This section compares the modelled effect of the different scenarios of green roofs to a scenario where Kvillebäcken would be built with roofs all painted white. The result for this comparison is shown as the energy flux in watts per square meter (Wm^-1) for Q_E and Q_H. The result (figure 15 & 16) shows that there is a slight increase in Q_E compared to the Base scenario when using high albedo roofs during the dry period. The main effect of high albedo roofs is shown in a decrease of Q_H.

Comparing the dry and the wet period, it becomes evident that during hot and sunny days the partitioning of energy into Q_E is small from both green and high albedo roofs (figure 15 & 16). This differs from the Q_H heat flux, which is highly reduced by high albedo roofs during the same conditions. The high albedo roof has the most effect during sunny and warm days, lowering the Q_H by approximately 50 Wm^-1. However, looking at the wet period there is only a slight reduction of the Q_H heat flux. The Q_E heat flux on the other hand is increased more during these conditions than during dry and warm conditions, meaning that green roofs have the largest cooling effect during wet conditions (figure 15 & 16).

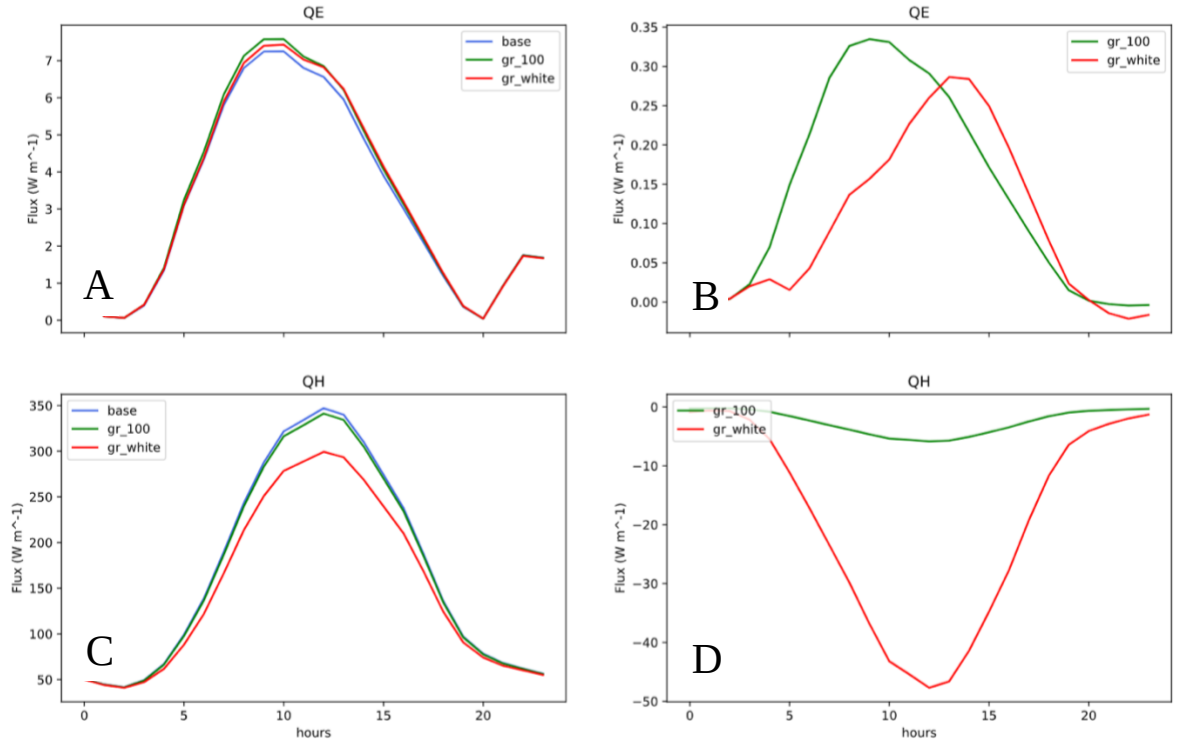

Figure 15: The average of daily energy flux for latent heat (Q_E) and sensible heat (Q_H) during a completely dry period. The period shown is 2018-07-20 until 2018-07-25. ***A****: Q_E flux,* ***B****: Q_E flux difference of scenarios from the Base scenario,* ***C****: Q_H flux,* ***D****: Q_H flux difference of scenarios from the Base scenario.*

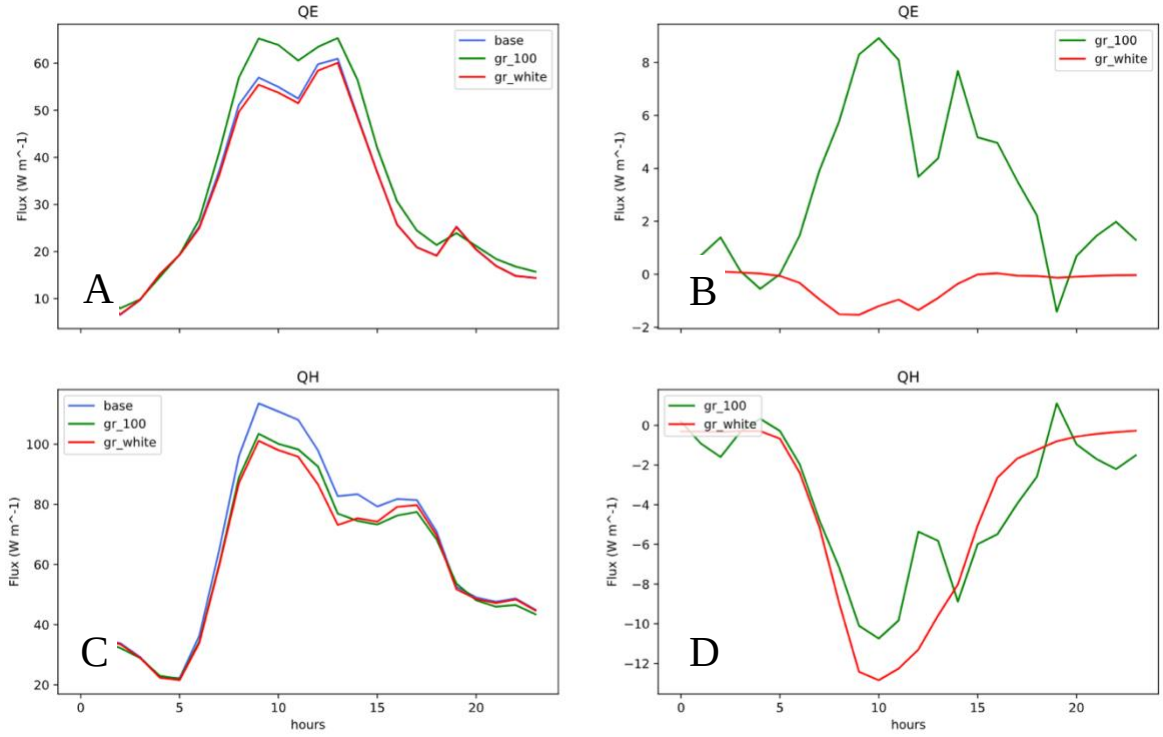

Figure 16: The average of daily energy flux for latent heat (Q_E) and sensible heat (Q_H) during the wet period. The period shown is 2018-10-02 until 2018-10-08. ***A****: Q_E flux,* ***B****: Q_E flux difference of scenarios from the Base scenario,* ***C****: Q_H flux,* ***D****: Q_H flux difference of scenarios from the Base scenario.*

6. Discussion

6.1. Partitioning of latent and sensible heat in Kvillebäcken with current BGI

The building structure of Kvillebäcken with a small fraction of vegetation, where the fact that Kvillebäcken is newly rebuilt and therefore the important evapotranspiration effect from large trees does not exist, gives a low overall latent heat flux. The current green roofs and rain gardens in Kvillebäcken have a limited influence on partitioning into latent heat, especially on days without precipitation (figure 9, 10, 11 & 12). During the dry period there are several days where there is no or a very small difference between the Base scenario and rain gardens and green roofs respectively, indicating that the current BGI in Kvillebäcken does not increase the partitioning of latent heat during these conditions. This is likely due to the building structure of Kvillebäcken with a large proportion of impermeable and dark surfaces, which mainly radiates sensible heat (Oke et al., 2017) contributing to warming of the nearby air.

6.2. Influence of rain gardens and additional water to green surfaces

Rain gardens are mainly built to retain runoff, to not overload the storm water systems (SMHI, 2018) but can evidently also have a small influence on the energy partitioning in an urban area. When increasing the surface area of rain gardens, there is a slight increase in the latent heat flux. The difference is at its maximum for the scenario with 30% rain gardens and differ approximately 25% from the Base scenario during days following a rain event (figure 9 & 10). The effect is short-term but it is evident that rain gardens to some extent have the potential to affect the latent heat flux, like all other vegetation in the urban area (Meili et al., 2020). This result is expected because of the rain garden's purpose of retaining excess water (SMHI, 2018), leading to an increased moisture availability and therefore also leading to potential for an increased latent heat flux. The strongest increase of the fraction of latent heat occurs after rainfall, but the largest need for urban cooling is during dry and warm periods (Gunawardena et al., 2017). When all building runoff is led to vegetated areas, and also to rain gardens, the increase of latent heat is enhanced further in comparison to the Base scenario. Again, this is a result of the increased water availability at the surface which increases the possibility for water to evaporate and thereby energy is partitioned into latent heat (Oke et al., 2017).

6.3. Influence of increased green roof cover

Increasing the green roof cover in Kvillebäcken increases the latent heat flux, where the effect lasts up to 24 hours. The greatest effect is reached by the scenario where green roofs cover 100% of the roof area. To implement green roofs on a building goes in line with what Oke et al. (2017) discusses on how neighborhoods should work to enhance or at least not worsen their surrounding microclimate, where green roofs can be seen to compensate for parts of the low urban latent heat flux (ibid.). The effect of increasing green roofs is smaller than changing land use from paved to grass, however it can be argued that since roof areas rarely compete with other interests of the city it is a more realistic measure to consider. When incorporating BGI in urban areas, it is preferable to retrofit already existing structures rather than creating new areas which compete with other interests in the urban environment (Calheiros & Stefanakis, 2021). Due to the availability of roof space it is also reasonable to suggest 100% green roof coverage or at least a large proportion of the total roof area in a similar future building project. The result demonstrates a clear difference between the scenarios, where 100% green roof coverage gives the larger increase of latent heat, beneficial for the reduction of temperatures in Kvillebäcken.

Looking at the green roof effect on the latent heat flux during the two periods of different weather conditions it is evident that green roofs have a larger influence during periods of more precipitation and that they do not have any effect during periods of drought (figure 11 & 12). This means that during heatwaves (which the July Case study period is an example of) when cooling is needed the most, green roofs have little or no effect on increasing the latent heat flux. Extensive green roofs generally have a higher drought tolerance than the other types of green roofs due to the selection of drought tolerant plants (Nagase & Dunnett, 2010). However, they can only withstand drought to a certain extent before the transpiration decreases and eventually the plants die meaning that the green roof no longer contributes to increasing the latent heat flux through transpiration (Al-Busaidi, Yamamoto, Tanak & Moritani, 2013). During periods of dry and hot weather, green roofs therefore do not contribute to cooling and it does not decrease heat stress and UHI efficiently in Kvillebäcken. The same result applies to all scenarios of green roof coverage, contradicting previous research, for example what Sun, Grimmond and Ni (2016) presents for a warm temperate monsoon climate.

6.4. Green roof and high albedo roof comparison

During hot and dry conditions green roofs have a low potential to increase latent heat and thereby to reduce urban temperature. High albedo roofs seem to have the largest effect on reducing the sensible heat flux during these conditions, which can lower the temperature in periods of extreme heat. Taken together with the lower cost of installation and small need for maintenance, cool roofs can according to the result of this thesis be more efficient when it comes to temperature reduction in urban areas (EPA, n.d). However, the high albedo roof lacks the multifunctionality of the green roof, such as aesthetic, ecosystem and rain retention values which makes the reasoning of Oke et al. (2017) regarding a mix of different solutions applicable on the Kvillebäcken example. A combination between high albedo roofs and green roofs could give a maximal effect with a variety of benefits.

6.5. Influence of land cover change – increased grass and decreased paved areas

Results of an increased fraction of grass in Kvillebäcken show an effect on the latent heat flux which is notable. It follows the pattern of other BGI, and the effect does not last long after rainfall events (figure 13 & 14.). Even though the effects of an increased grass fraction, and as a result also less paved surface, gives quite a large effect on the latent heat flux it can be questioned whether it is actually a reasonable scenario for an area like Kvillebäcken. The scenarios demand a drastic change in how the area is built and even if the amount of grass could be increased somewhat, it is not likely that almost 50% of the surface area in Kvillebäcken would be made up of grass. Grass competes with many other interests on ground level and in an urban environment, such as roads and buildings, and cannot extend into these fractions since they are the foundation of urbanity. The results suggest that for future constructions of areas similar to Kvillebäcken should focus on maximizing grass areas where possible due to the high potential of energy partitioning into latent heat flux. This should be done together with other BGI for a maximal latent heat increase (Oke et al., 2017).

Further, the effect on the latent heat flux of a change land cover is largest within the 24 hours after a rainfall event which suggests that water availability near the surface of soils is crucial in order for energy to be partitioned into latent heat in (Caporali & Civile, 1999). For the dry period, water becomes unavailable for evaporation within 24 hours, where some of the water most probably has evaporated giving an increased fraction of latent heat and some water becomes bound to the soil (Brogowski & Kwasowski, 2015). Moist grass surfaces give a higher

partitioning into latent energy, which could be distributed also to surrounding areas depending on the urban structure and wind circumstances (Oke et al., 2017).

6.5. Future research

The effect of precipitation on the partitioning of energy is clearly visible for all scenarios and for both rain gardens and green roofs. This suggests that the water availability is the crucial factor for an increase of latent heat flux and that the BGI in Kvillebäcken has little or no effect in periods of drought. Water availability and cooling could be increased through irrigation of vegetated areas, which in studies of green roofs has been seen to increase cooling potential (Tsang & Jim, 2016; Van Mechelen et al., 2015). It would therefore be interesting to investigate the potential of BGI with irrigation in Kvillebäcken to understand the effect of a constant supply of water through irrigation and how that could increase the latent heat flux.

Further, SUEWS works at a neighborhood scale but the effects on the heat fluxes seen in the smaller scale can have an effect also on a city scale (Susca et al., 2011). Through exchange between the atmospheric layers above the urban area, the effect of energy partitioning changes can affect other areas as well. Oke et al. (2017) demonstrate how the cooling effect of vegetated areas can be spread to the surroundings. Gunawardena et al. (2017) stated that BGI can increase the convection through an increased roughness and thereby increases the connection to the UBL which moves the cooling effect from a micro scale to a city-wide scale, meaning that the effect seen in Kvillebäcken potentially could reduce temperatures also in the neighboring parts of Gothenburg. Finally, assuming that several neighborhoods within an urban area increases both BGI presence and possibly also high albedo roofs, it will increase the all over latent heat flux of the urban area (Susca et al., 2011). Thus, more research is needed on how BGI can affect energy partitioning, not only on a micro scale but also on a city scale.

6.6. Uncertainties

This thesis has used an energy and water flux model as a method of investigating the potential of increasing the latent heat flux and reducing temperatures in Kvillebäcken. As for all models, it implies some simplifications of reality. One important parameter, plant transpiration, has been overlooked due to SUEWS modelling possibilities where the way green roofs are represented (section 4.1.7) does only use evaporation from green roofs and does not account for transpiration. Meili et al. (2020) states that this is an important parameter and the result in

this thesis could therefore be slightly underestimating the cooling potential of green roofs. It would be beneficial to compare the result in SUEWS to the way green roofs are modelled in Meili et al (2020), in order to investigate to what extent transpiration affects the temperature reducing effect of green roofs.

Further, the result does not account for the combined effect of rain gardens and green roofs but models them separately. It would be beneficial to further investigate the interplay between the two types of BGI to see if the water retention of the green roof possibly could slow the water access to rain gardens down, and thereby prolong the effect from a rainfall event. It would also be useful to look at an extended period of time and to not use an anomalous year weatherwise. The result concludes that the effect of BGI on the latent heat flux during the unusually warm and dry period of 2018 was small, but it is also important to recognize that BGI could have a larger influence during a year that is more normal in temperature and precipitation amounts.

7. Conclusion

Both rain gardens and green roofs have the potential to affect energy partitioning and can increase the fraction of latent heat in the urban environment, especially in wet periods. Both types of BGI have a low potential to affect the latent heat flux during periods of dry weather and are therefore not an efficient measure to lower temperatures during these conditions. Water availability and an increased latent heat flux is closely related, and measures to retain water at surface level is crucial in order for rain gardens, green roofs and grass areas to have a cooling influence through latent heat on the nearby air mass. The high albedo roofs have shown to be more efficient during periods of urgent need, such as during the heatwave period of July 2018 where it efficiently decreases the sensible heat flux and thereby lower temperatures. However, a combination of BGI and high albedo surfaces would probably reach the largest overall benefits for an urban area that needs to counteract the issues of high temperatures enhanced by the urban structure and climate change. Finally, the effects on the energy partitioning from rain gardens, green roofs and high albedo roofs can have widespread effects on neighboring areas as well as the total Urban Energy Balance.

8. References

Al-Busaidi, A., Yamamoto, T., Tanak, S., & Moritani, S. (2013). Evapotranspiration of Succulent Plant (Sedum aizoonvar. floibundum). Evapotranspiration-An Overview, 242-257.

Alexander, P. J., Fealy, R., & Mills, G. M. (2016). Simulating the impact of urban development pathways on the local climate: A scenario-based analysis in the greater Dublin region, Ireland. *Landscape and Urban Planning*, *152*, 72–89. https://doi.org/10.1016/j.landurbplan.2016.02.006

Arabi, R., Shahidan, M., Mohd Shariff, M., Ja'afar, M., & Rakhshandehroo, M. (2015). Considerations for plant selection in green roofs. *ALAM CIPTA, International Journal on Sustainable Tropical Design Research & Practice*, *8*(spec.3), 10–17.

Best, M. J., & Grimmmmond, C. S. B. (2015). Key conclusions of the first international urban land surface model comparison project. *Bulletin of the American Meteorological Society*. https://doi.org/10.1175/BAMS-D-14-00122.1

Bergroth, C. (2019). *Uncovering population dynamics using mobile phone data: The case of Helsinki Metropolitan area (*Master Thesis). Helsinki: Department of Geoscience and Geography. Avaliable: https://helda.helsinki.fi/handle/10138/302228

Brogowski, Z., & Kwasowski, W. (2015). An attempt of using soil grain size in calculating the capacity of water unavailable to plants. *Soil Science Annual*, *66*(1), 21–28. https://doi.org/10.1515/ssa-2015-0015

Calheiros, C. S. C., & Stefanakis, A. I. (2021). Green Roofs Towards Circular and Resilient Cities. *Circular Economy and Sustainability*. https://doi.org/10.1007/s43615-021-00033-0

Capener, C.-M., Pettersson Skog, A., Emilsson, T., Malmberg, J., Jägerhök, T., Edwards, Y., & Månsson, H. (2017). *Grönatakhandboken Kvalitetssäkrade systemlösningar för gröna anläggningar / tak nolltolerans mot läckage*. http://gronatakhandboken.se/wp-content/uploads/2017/05/Gronatakhandboken-Vagledning-Lowres.pdf

Caporali, E., & Civile, I. (1999). *using adjoint-state surface energy balance T • - < T • > = x / top • C • • AT • = P •. 35*(10), 3115–3125.

Christen, A., & Vogt, R. (2004). Energy and radiation balance of a central European City. *International Journal of Climatology*. https://doi.org/10.1002/joc.1074

Conservation International (n.d). Green-Gray infrastructure - Working with nature to protect vulnerable communities. Retrieved 2021-04-28 from https://www.conservation.org/projects/green-gray-infrastructure

Coutts, A. M., Beringer, J., & Tapper, N. J. (2007). Impact of increasing urban density on local climate: Spatial and temporal variations in the surface energy balance in Melbourne, Australia. Journal of Applied Meteorology and Climatology, 46(4), 477–493. https://doi.org/10.1175/JAM2462.1

European commission (2019). *Guidance on a strategic framework for further supporting the deployment of EU-level green and blue infrastructure.* Brussels: European Commission.

Erell, E., Pearlmutter, D., & Williamson, T. (2010). Urban microclimate: designing the spaces between buildings. Routledge.

Finewood, M. H., Matsler, A. M., & Zivkovich, J. (2019). Green Infrastructure and the Hidden Politics of Urban Stormwater Governance in a Postindustrial City. *Annals of the American Association of Geographers*, *109*(3), 909–925. https://doi.org/10.1080/24694452.2018.1507813

Gkatsopoulos, P. (2017). A Methodology for Calculating Cooling from Vegetation Evapotranspiration for Use in Urban Space Microclimate Simulations. *Procedia Environmental Sciences*, *38*, 477–484. https://doi.org/10.1016/j.proenv.2017.03.139

Grimmond, C. S. B. (1992). The suburban energy balance: Methodological considerations and results for a mid-latitude west coast city under winter and spring conditions. *International Journal of Climatology*, *12*(5), 481–497. https://doi.org/10.1002/joc.3370120506

Gothenburg Municipality (2015). *Undvik översvämning – gör en regnrabatt.* Gothenburg: Gothenburg Municipality.

Gothenburg Municipality (2020). *Kvillebäcken.* Retrieved 2021-05-03 from https://stadsutveckling.goteborg.se/projekt/kvillebacken/

Gothenburg Municipality (2021). *Så ser Göteborg ut om 20 år.*. Retrieved 2021-05-03 from https://stadsutveckling.goteborg.se/nyheter/sa-ser-goteborg-ut-om-20-ar/

Gothenburg Minucipality (n.d) *Regnrabatt minskar översvämningsrisken.* Retrieved 2021-04-28 from https://goteborg.se/wps/portal/start/miljo/det-har-kan-du-gora/regnrabatter?uri=gbglnk%3A2015512123814

Gothenburg University. (2021). *Multifunctional blue-green infrastructure - optimizing socio-cultural and environmental aspects for sustainable urban development.* Retrieved 2021-04-27 from https://www.gu.se/forskning/multifunctional-blue-green-infrastructure-optimizing-socio-cultural-and-environmental-aspects-for-sustainable-urban-development-0

Springer International Publishing AG, part of Springer Nature 2018 G. P. O. Reddy, S. K. Singh (eds.), Geospatial Technologies in Land Resources Mapping, Monitoring and Management, *Geotechnologies and the Environment* 21, https://doi.org/10.1007/978-3-319-78711-4_11

Gunawardena, K. R., Wells, M. J., & Kershaw, T. (2017). Utilising green and bluespace to mitigate urban heat island intensity. *Science of the Total Environment*, *584–585*, 1040–1055. https://doi.org/10.1016/j.scitotenv.2017.01.158

Hathway, E. A., & Sharples, S. (2012). The interaction of rivers and urban form in mitigating the Urban Heat Island effect: A UK case study. *Building and Environment*, *58*, 14-22.

Heaviside, C., Macintyre, H., & Vardoulakis, S. (2017). The Urban Heat Island: Implications for Health in a Changing Environment. *Current Environmental Health Reports*, *4*(3), 296–305. https://doi.org/10.1007/s40572-017-0150-3

IPCC, 2014: Climate Change 2014: Synthesis Report. Contribution of Working Groups I, II and III to the Fifth Assessment Report of the Intergovernmental Panel on Climate Change [Core Writing Team, R.K. Pachauri and L.A. Meyer (eds.)]. IPCC, Geneva, Switzerland, 151 pp.

Johansson, S. (2017) The influence of land cover on urban energy balance in Gothenburg (Master Thesis). Department of Earth Sciences. Available: https://studentportal.gu.se/digitalAssets/1686/1686482_b987.pdf

Järvi, L., Grimmond, C. S. B., & Christen, A. (2011). The surface urban energy and water balance scheme (SUEWS): Evaluation in Los Angeles and Vancouver. Journal of Hydrology, 411(3-4), 219-237.

Järvi, L., Grimmond, C. S. B., Taka, M., Nordbo, A., Setälä, H., & Strachan, I. B. (2014). Development of the Surface Urban Energy and Water Balance Scheme (SUEWS) for cold climate cities. *Geoscientific Model Development*, *7*(4), 1691–1711. https://doi.org/10.5194/gmd-7-1691-2014

Kabisch, N., Korn, H., Stadler, J., & Bonn, A. (2017). *Nature-Based Solutions to Climate Change Adaptation in Urban Areas—Linkages Between Science, Policy and Practice* (pp. 1–11). https://doi.org/10.1007/978-3-319-56091-5_1

Kati, V., & Jari, N. (2016). Bottom-up thinking-Identifying socio-cultural values of ecosystem services in local blue-green infrastructure planning in Helsinki, Finland. *Land*

Use Policy, *50*, 537–547. https://doi.org/10.1016/j.landusepol.2015.09.031
Konarska, J., Lindberg, F., Larsson, A., Thorsson, S. & Holmer, B. (2013). *Transmissivity of solar radiation through crowns of single urban trees—application for outdoor thermal comfort modelling.* Theoretical and Applied Climatology. 117. 1-14. 10.1007/s00704-013-1000-3.
MacIvor, J. S., & Lundholm, J. (2011). Performance evaluation of native plants suited to extensive green roof conditions in a maritime climate. *Ecological Engineering*, *37*(3), 407–417. https://doi.org/10.1016/j.ecoleng.2010.10.004
Meili, N., Manoli, G., Burlando, P., Bou-Zeid, E., Chow, W. T. L., Coutts, A. M., Daly, E., Nice, K. A., Roth, M., Tapper, N. J., Velasco, E., Vivoni, E. R., & Fatichi, S. (2020). An urban ecohydrological model to quantify the effect of vegetation on urban climate and hydrology (UT&C v1.0). *Geoscientific Model Development*, *13*(1), 335–362. https://doi.org/10.5194/gmd-13-335-2020
Miao S G, Chen F. 2014. Enhanced modeling of latent heat flux from urban surfaces in the Noah/single-layer urban canopy coupled model. Science China: Earth Sciences, 57: 2408–2416, doi: 10.1007/s11430-014-4829-0
Muthanna, T. M., Viklander, M., & Thorolfsson, S. T. (2008). Seasonal climatic effects on the hydrology of a rain garden. Hydrological Processes: An International Journal, 22(11), 1640-1649.
Muthanna, T. M. (2010). Seasonal climatic effects on the hydrology of a rain garden. *Okt 2005 Abrufbar Uber Httpwww Tldp OrgLDPabsabsguide Pdf Zugriff 1112 2005*, Muthanna, T. M., Viklander, M., & Thorolfsson, S. T. (2008). Seasonal climatic effects on the hydrology of a rain garden. Hydrological Processes: An International Journal, 22(11), 1640-1649.*2274*
Nagase, A., & Dunnett, N. (2010). Drought tolerance in different vegetation types for extensive green roofs: Effects of watering and diversity. *Landscape and Urban Planning*, *97*(4), 318–327. https://doi.org/10.1016/j.landurbplan.2010.07.005
Nikon (n.d.) *Forestry Pro.* Retrieved 2021-05-03 from https://imaging.nikon.com/lineup/sportoptics/laser/forestrypro/
Oke, T. R. (1976). The distinction between canopy and boundary-layer urban heat Islands. *Atmosphere*, *14*(4), 268–277. https://doi.org/10.1080/00046973.1976.9648422
Oke, T.: Boundary Layer Climates, Routledge, London, UK, 1987. Punkka, A. J. and Bister, M.: Occurrence of summertime convec- tive precipitation and mesoscale convective systems in Finland during 2000-01, Mon. Weather Rev., 133, 362–373, 2005.
Oke, T.R., Mills, G., Christen, A. & Voogt, J. A. (2017). *Urban Climates.* Cambridge: Cambridge University Press.
Oliver J.E. (2005) Maritime Climate. In: Oliver J.E. (eds) Encyclopedia of World Climatology. Encyclopedia of Earth Sciences Series. Springer, Dordrecht. https://doi.org/10.1007/1-4020-3266-8_131
Pandas Manual (2021). *pandas.DataFrame.interpolate.* Retrieved 2021-05-03 from https://pandas.pydata.org/pandas-docs/stable/reference/api/pandas.DataFrame.interpolate.html
SCB (2020). *Folkmängd, top 50.* Retrieved 2021-05-03 from https://www.scb.se/hitta-statistik/statistik-efter-amne/befolkning/befolkningens-sammansattning/befolkningsstatistik/pong/tabell-och-diagram/topplistor-kommuner/folkmangd-topp-50/
Sailor, D. J., & Lu, L. (2004). A top-down methodology for developing diurnal and seasonal anthropogenic heating profiles for urban areas. *Atmospheric Environment*, *38*(17), 2737–2748. https://doi.org/10.1016/j.atmosenv.2004.01.034
Simperler, L., Ertl, T., & Matzinger, A. (2020). *Spatial Compatibility of Implementing*

Nature-Based Solutions for Reducing Urban Heat Islands and Stormwater Pollution. https://doi.org/10.3390/su1215596
SUEWS Manual A (2019). *Introduction.* Retrieved 2021-05-03 from https://suews.readthedocs.io/en/develop/introduction.html
SUEWS Manual B (2019). *SUEWS_NonVeg.txt.* Retrieved 2021-05-17 from https://suews.readthedocs.io/en/latest/input_files/SUEWS_SiteInfo/SUEWS_NonVeg.html
SUEWS Manual C (2019). *SUEWS_Veg.txt.* Retrieved 2021-05-17 from https://suews.readthedocs.io/en/latest/input_files/SUEWS_SiteInfo/SUEWS_Veg.html
Sun, R., & Chen, L. (2012). How can urban water bodies be designed for climate adaptation? *Landscape and Urban Planning*, *105*(1–2), 27–33. https://doi.org/10.1016/j.landurbplan.2011.11.018
Sun, T., Grimmond, C. S. B., & Ni, G. (2016). How do green roofs mitigate urban thermal stress under heat waves? *Journal of Geophysical Research Atmospheres*, *175*(21), 5320–5335. https://doi.org/10.1038/175238c0
Sun, T., & Grimmond, S. (2019). A Python-enhanced urban land surface model SuPy (SUEWS in Python, v2019.2): Development, deployment and demonstration. *Geoscientific Model Development*, *12*(7), 2781–2795. https://doi.org/10.5194/gmd-12-2781-2019
Susca, T., Gaffin, S. R., & Dell'Osso, G. R. (2011). Positive effects of vegetation: Urban heat island and green roofs. *Environmental Pollution*, *159*(8–9), 2119–2126. https://doi.org/10.1016/j.envpol.2011.03.007
Swedish Meteorological and Hydrological Institute (SMHI) (2017) *Normal uppmätt årsnederbörd, medelvärde 1961-1990*. Retrieved 2021-04-28 https://www.smhi.se/data/meteorologi/nederbord/normal-uppmatt-arsnederbord-medelvarde-1961-1990-1.4160
Swedish Meteorological and Hydrological Institute (SMHI) (2018). *Regnrabatter i Göteborg.* Retrieved 2021-04-28 from https://www.smhi.se/klimat/klimatanpassa-samhallet/exempel-pa-klimatanpassning/regnrabatter-i-goteborg-1.117300
Swedish Meteorological and Hydrological Institute (SMHI) (2019). *Gröna tak, fördjupning.* Retrieved 2021-04-28 from https://www.smhi.se/klimat/klimatanpassa-samhallet/exempel-pa-klimatanpassning/grona-tak-fordjupning-1.116956
Swedish Meteorological and Hydrological Institute (SMHI) (nd.). *Förändring av årsnederbörden i Västra Götalands län, scenario RCP4,5.* Retrieved 2021-05-03 from https://www.smhi.se/klimat/framtidens-klimat/klimatscenarier/sweden/county/vastra-gotalands/rcp45/year/precipitation
Swedish Meteorological and Hydrological Institute (SMHI) (n.d.) *Data*. Retrieved 2021-05-07 from https://www.smhi.se/data
Taha, H. (1997). Urban climates and heat islands: albedo, evapotranspiration, and anthropogenic heat. *Energy and Buildings*, *25*(2), 99–103. https://doi.org/10.1016/S0378-7788(96)00999-1
Thorsson, S., Rayner, D., Lindberg, F., Monteiro, A., Katzschner, L., Lau, K. K. L., ... & Holmer, B. (2017). Present and projected future mean radiant temperature for three European cities. International journal of biometeorology, 61(9), 1531-1543.
Tsang, S. W., & Jim, C. Y. (2016). Applying artificial intelligence modeling to optimize green roof irrigation. *Energy and Buildings*, *127*, 360–369. https://doi.org/10.1016/j.enbuild.2016.06.005
UMEP Manual A (2020). *SUEWS Prepare.* Retrieved 2021-05-03 https://umep-docs.readthedocs.io/en/latest/pre-processor/SUEWS%20Prepare.html
UMEP Manual B (2020). *Meteorological Data: MetPreprocessor.* Retrieved 2021-05-03

https://umep-docs.readthedocs.io/en/latest/pre-processor/Meteorological%20Data%20MetPreprocessor.html
United States Environmental Protection Agency (EPA). (nd.). *Using Green Roofs to Reduce Heat Islands.* Retrieved 2021-04-05 from https://www.epa.gov/heatislands/using-green-roofs-reduce-heat-islands
Van Mechelen, C., Dutoit, T., & Hermy, M. (2015). Adapting green roof irrigation practices for a sustainable future: A review. In *Sustainable Cities and Society* (Vol. 19, pp. 74–90). Elsevier Ltd. https://doi.org/10.1016/j.scs.2015.07.007
VA-guiden (2020). *Recept på regnrabatt*. Retrieved 2021-04-28 from https://vaguiden.se/2020/08/recept-pa-regnrabatt/
Venvik, G., & Boogaard, F. C. (2020). Infiltration capacity of rain gardens using full-scale test method: Effect of infiltration system on groundwater levels in Bergen, Norway. *Land*, *9*(12), 1–18. https://doi.org/10.3390/land9120520
Voelker, S., Baumeister, H., Classen, T., Hornberg, C., & Kistemann, T. (2013). Evidence for the temperature-mitigating capacity of urban blue space—A health geographic perspective. Erdkunde, 355-371.
Ward, H. C., Kotthaus, S., Järvi, L., & Grimmond, C. S. B. (2016). Surface Urban Energy and Water Balance Scheme (SUEWS): Development and evaluation at two UK sites. *Urban Climate*, *18*, 1–32. https://doi.org/10.1016/j.uclim.2016.05.001 Al-Busaidi, A., Yamamoto, T., Tanak, S., & Moritani, S. (2013). Evapotranspiration of Succulent Plant (Sedum aizoonvar. floibundum). Evapotranspiration-An Overview, 242-257.
Wing, C. (2021). *Evaluating Greeney in Urban Typologies* (Master Thesis). Gothenburg: Department of Earth Sciences.
World Health Organization. (2017). *Urban green space interventions and health: A review of impacts and effectiveness.* Copenhagen: World Health Organization.
Yu, Z., Yang, G., Zuo, S., Jørgensen, G., Koga, M., & Vejre, H. (2020B). Critical review on the cooling effect of urban blue-green space: A threshold-size perspective. Urban Forestry and Urban Greening, 49(February), 126630. https://doi.org/10.1016/j.ufug.2020.126630
Žuvela-Aloise, M., Koch, R., Buchholz, S., & Früh, B. (2016). Modelling the potential of green and blue infrastructure to reduce urban heat load in the city of Vienna. Climatic Change, 135(3), 425-438.